DESIGN AND CONSTRUCTION OF A PARALLEL PLATE IONIZATION CHAMBER FOR DOSIMETRY IN CONVENTIONAL RADIOGRAPHY

A THESIS SUBMITTED TO THE

DEPARTMENT OF MEDICAL PHYSICS

SCHOOL OF NUCLEAR AND ALLIED SCIENCES

UNIVERSITY OF GHANA, LEGON

BY

ALI MORROW FATORMAH

(10703745)

BSc. Kwame Nkrumah University of Science and Technology, 2014

IN PARTIAL FULFULMENT OF THE REQUIREMENT FOR THE AWARD OF

MASTER OF PHILOSOPHY DEGREE

IN

MEDICAL PHYSICS

OCTOBER, 2020

DECLARATION

I hereby declare that I have wholly undertaken this project under the supervision of Dr. S. N. A Tagoe and Dr. F. Hasford and no other part or whole of this work has been submitted for any degree elsewhere in another university, References of other peoples' work have been duly acknowledged.

……06/08/2021……..

Ali Morrow Fatormah — Date

(Student)

……19/08/2021…….

Dr. Samuel Nii Adu Tagoe — Date

(Principal Supervisor)

……19/08/2021……

Dr Francis Hasford — Date

(Co-Supervisor)

ABSTRACT

The main objective of every radiodiagnostic procudure is to produce an informative image with minimum radiation exposure to patients. To be able to minimize dose to patients, and ensure image quality, there must be a regular quality control on the entire X-ray systems, which involves routine measurement of exposure and exposure rate. The most employed dosimeters for the adjustment and control measurements is the parallel plate ionization chamber. It is less intrinsic to energy dependence, hence mostly recommended for low dose rate measurement. It is in view of this, that a portable, and less expensive detector (parallel plate ionization chamber) has been designed and constructed for dosimetry in diagnostic radiography.The chamber comprises of a body made of Perspex (1.7 mg/cm^2), a bias electrode made of copper plate, a measuring electrode made of an aluminium plate, guard rings made of an aluminium plate an entrance window made of a paper coated with graphite (shading the paper with HB pencil until the paper became electrically conductive) with the uncoated side pasted to a piece of unexposed developed radiographic film. The chamber has a sensitive volume of 2.8 cc which was vented to the environment. The operational bias voltage of the constructed ionization chamber was found to range from 200 V – 400 V. Two different conceptual designs were developed and evaluated. The concept with the highest overall utility value was selected and developed. The completed chamber was subjected to several performance characteristic and quality control tests: energy dependence, response reproducibility and constancy, angular dependence, response linearity and leakage characteristics. The chamber was cross calibrated against diagnostic multimeter (Piranha) with traceability to a secondary standard dosimetry laboratory (Swedac. Ackredictering,

Sweden) and found to have a calibration coefficient (N_K) of 1.7 x10^9 mGy/A. Beam quality correction factor for chamber could be expressed with a fourth degree polynomial equation in terms of HVL (mmAl) using 100 kVp and 20 mAs (200 mA) as the reference exposure parameters. Response reproducibility and constancy, angular dependence, response linearity were all within the International Electrotechnical Commission (IEC) 61674 stipulated limit. A maximum deviation of 8.6% was observed at 90^O clockwise of the gantry angle. This was as a result of cable leakage. A parallel plate ionization chamber has successfully been designed and developed and is applicable in a range of 50 -130 kVp.

DEDICATION

This project, is first and foremost dedicated to the Almighty Allah who has been my strength and source of knowledge throughout the entire program. To my late father, Kofi Ali Fatormah, though you are gone, your counsel on the ethos of education still lives. May the mercy of Allah be with you.

ACKNOWLEDGEMENTS

My profound and sincere gratitude goes to my able supervisors, Dr. Samuel Nii Adu Tagoe and Dr. Francis Hasford for their excellent supervisory role and immense technical contribution towards the success of this project.

Special appreciation to Ghana Education Trust Fund (GETFund) for offering me full scholarship for this study.

Special acknowledgement goes to my lovely wife, Hawaawu, my daughter Zaye-nabe, and my two sons Baba and Ziad for their understanding during what has been undeniably the uttermost fortitude of my physical absence during my study.

Again, I would like to thank the staff of the Medical Physics Unit of the National Radiotherapy Oncology and Nuclear Medicine Centre, (NRONMC), especially Mr. Francis Doughan for his assistance.

My heartfelt gratitude goes to Dr. Theresa Dery and Mr. Ernest Eduful, I am indeed very grateful to you for your assistance.

Finally, my greatest thank goes to the Almighty Allah for his mercy, guidance and protection in the course of this study.

TABLE OF CONTENT

TABLE OF FIGURES

LIST OF TABLES

LIST OF ABBREVIATIONS

AAPM	American Association of Physicist in Medicine
ADCL	Accredited Dosimetry Calibration Laboratory
AFD	Axis to Film Distance
CAD	Computer Aided Design
CT	Computed Tomography
EMF	Electromotive Force
FAD	Focal spot to Axis Distance
f_{ion}	Ion Collection Efficiency
GETFund	Ghana Education Trust Fund
HVL	Half Value Layer
IAEA	International Atomic Energy Agency
IEC	International Electrotechnical Commision
Kpol	Polarity Effect
k_Q	Beam Quality Correction Factor,
Ks	Saturated Factor
K_{TP}	Corrected Temperature and Pressure,
kVp	Kilo Voltage Peak
LCD	Liquid Crystal Display
Linac	Linear Accelerator
M_{corr}	Corrected Chamber Responses
mGy	Milli Gray
M_{uncorr}	Uncorrected Chamber Response
N_k	Calibration Coefficient

NRONMC	National Radiotherapy Oncology and Nuclear Medicine Centre
pA	Pico Ampere
PMMA	Polymethylmethacrylate
SSDL	Secondary Standard Dosimetry Laboratory

CHAPTER ONE

INTRODUCTION

1.1 Background

In medicine, the most common artificial source of public exposure to ionizing radiation is diagnostic X-ray and this is due to its extensive use in most diagnostic facilities. In Ghana, thousands of diagnostics X-ray procedures are carried out each year. Despite the fact that radiation exposure connected with these procedures is unavoidable, there are various means to reduce it as much as possible (Halato et al., 2008). To be able to minimize dose to patients, and ensure image quality, there must be a regular quality control on the entire X-ray systems, which involves routine measurement of air kerma and exposure rate.

Parallel plate ionization chambers are one of most employed dosimeters for the adjustment and control measurements in achieving the required accuracy (IEC, 2013). The estimation of the skin entrance dose depends largely on the air kerma and the beam quality. The right backscatter factor is applied in order to convert the air kerma into skin entrance dose. (Alessandro & Caldas, 2008).

The goal of every radio-diagnostic examination is to provide a clinical informative radiographic image while minimizing dose to patients. Periodic quality control is a requisite for ensuring the safe use of X-ray equipment facility (Alessandro & Caldas, 2008).

The demand of diagnostic radiological services in a developing country like Ghana will keep on increasing with complex quality control, quality assurance, patient dose management and radiation protection challenges (Inkoom et al., 2011).

In considering these, the utmost objective should be arriving at a diagnostic image that satisfies clinical requirements whiles ensuring minimum patient dose.

Again, the critical adjustment of parameters such as tube voltage (kVp), air kerma reproducibility and linearity with the tube current product-exposure time (mAs) are particularly very important. Also, a better understanding of the relationship between the image and these parameters, and the measurement of these characteristics with the right tools is necessary. Over time, characteristics of these parameters may change, this calls for periodic tests to be performed in order to avoid downtime and ensure that all diagnostic X-ray machines are accurately calibrated and function at optimal level and that the procedures and images are safe and informative (Hasford, 2018).

Ionization chambers are used in the determination of the incident air kerma, reproducibility, linearity of air kerma and HVL as function of the mAs. Calibration of the output of photon beam produced by any X-ray system to achieve optimization of Dose to patients is by the use of an ionization chamber (Parallel plate ionization chamber) (Podgorsak, 2005). Parallel plate ionization chambers, also called surface ionization chambers, depending on their sensitive volume and characteristics, have different geometries. In order to accept a measurement as valid, it is important for the user to consider and well understand the specifications for the design of an ionization chamber. (Alessandro and Caldas, 2008).

This study seeks to design and construct a vented parallel plate type ionization chamber and investigate whether the chamber satisfies the routine criteria for calibration of diagnostic X-ray machines (conventional radiography) in the clinical setting.

1.2. Statement of the problem

Delivering clinical informative radiographic images while minimizing dose to patients are the primary goals of any radio-diagnostic program. In view of this, the International Atomic Energy Agency (IAEA) recommends at least two ionization chambers for a diagnostic center. This is a challenge in most diagnostic centers in developing countries due to cost implications.

Due to the significance of quality control in diagnostic imaging, it is recommended that the staff at the facilities should ensure a routine review, for instance quarterly reviews, of the control tests, data and images, but this is not the case of most diagnostic centers in Ghana, due to cost and the health implications cannot be overemphasized. Preliminary checks at some of the major medical imaging facilities in Ghana reveal a lack of the availability of parallel plate ionization chamber. As such researchers, who need ionization chambers to perform dosimetry needs, always have to rely on Radiation Protection Institute (RPI) for their limited dosimeters for their studies. In X-ray systems, Parallel plate ionization chambers are the most preferred choice for quality control because, they are used for small field dosimetry or low dose rate measurements. In view of this, there is the need to find a less expensive vented parallel plate ionization chamber which is environmentally friendly for daily QCs.

1.3 Aims and Objectives

The main objective of the study is to design and fabricate a vented parallel plate ionization chamber from available materials for quality control in X-ray systems

The specific objectives are to:

- Design and construct a vented parallel plate ionization chamber from available materials.
- Calibration of the constructed ionization chamber for X-ray beam
- Establishing the traceability of the newly constructed chamber, by cross calibrating it with another ionization chamber whose traceability is to a secondary standard dosimetry laboratory (SSDL).
- Determination of calibration coefficient of the chamber to enable reference dosimetry measurement with the chamber.

1.4 Scope and delimitation

The scope of this project is limited to the designing, construction and testing of a portable vented parallel plate ionization chamber and validating it against those stipulated in the International Electrotechnical Commission (IEC) 61674, 2013, for standard ionization chambers. It also include the selection of material, manufacturing processes and cost analysis into materials.

Measurements and procedures to ensure clinical application of the constructed waterproof portable parallel plate ionization chamber have been considered.

1.5 Thesis organization

The project is organized into five chapters. Chapter 1 talks about the Introduction which includes the study background, Problem statement, aims and objectives, significance of the project and the organization of the thesis report. Chapter 2 discusses literature and theories on the various types of ionization chambers. Chapter 3 centres on the materials and methods adopted for the study. It highlights the conceptual design of the parallel-plate ionization chamber, processes of manufacturing, design calculations and parts and their functions. Chapter 4 presents the results for the construction and findings for pre-evaluations measurements of the newly constructed ionization chamber. Chapter 5pesents, conclusion of this project and suggested recommendations for further work.

CHAPTER TWO

LITERATURE REVIEW

2.1 Dosimetry in diagnostic radiology

Dosimetry is an integral component of diagnostic radiology and it requires the use special instruments. The construction and performance of such instruments must correspond to the demands of the clinical situation. Also, specialized techniques and knowledge may be needed in the use and the interpretation of the result obtained from such instrumentation (IAEA, TRS No.457).

Annals of the American Association of Physicist in Medicine (AAPM) explains that, the performances of diagnostic dosimeters, categorized the measurements into two: those used to evaluate the risks of radiation damage from X-ray examination and those performed as part of quality assurance programs and radiation surveys of workplace and areas the general public occupies. Also, the quality assurance measurements can be grouped into two: the one used for establishing absolute values of the experimented parameters and those used in comparison with the baseline values established for the same unit or with parameter values determined for another unit. (AAPM, 1992)

The most important use of dosimetric quantities in diagnostic radiology is the protection of staff and patients from ionizing radiation. Nonetheless, the absorbed dose is the amount that best shows the effects of radiation on products or on humans, and thus all the amounts associated with safety are centered on it. (IAEA, TRS No. 457, 2007).

The derivatives of absorbed dose include air kerma, fluence or equivalent dose. The absorbed dose is the amount of energy absorbed per unit mass. It is the quantity of most interest in diagnostic radiology. From experiments performed on ionization chambers,

absorbed dose to air (D_{air}) is the quantity used to compare the responses of the different detectors and is expressed as

$$D_{air} = \frac{Q}{m} * \text{W} \qquad (2.1)$$

Using the charge (Q) measured by the electrometer in Coulombs and the mass (m) of air in kg, and mean energy (W) required to produce an ion pair in air per unit charge (e). Currently, the value of W for dry air is 33.97 eV/ion pair or 33.97 J/C, the SI unit of absorbed dose is the gray, abbreviated Gy.

It is important to correct the mass of air for temperature and pressure using the Ideal Gas Law,

$$\rho_{air} = \frac{P}{RT} \qquad (2.2)$$

Where ρ_{air} is the density of air, P is the air pressure, R is the ideal gas constant for air, and T is temperature. Then the mass of air is

$$mass_{air} = \rho\, V, \qquad (2.3)$$

Where V is the volume of the air cavity.

Khan (2010), expressed the quantity kerma (K), as the quotient of the summation of the primary kinetic energies of all the charged ionizing particles released by uncharged particles, dE_{tr} in a given material of mass dm.

$$\text{K} = \frac{dEtr}{dm} \qquad (2.4)$$

Khan (2010), defined fluence,Φ as the number of particles or photons, traversing a medium. ICRU formal definition for fluence, Φ is:

$$\Phi A = \frac{dN}{dA} \tag{2.5}$$

Where dN represent the total sum of particles directed on a sphere and dA is the cross sectional area.

Evaluating of the health effect of radiation from X-ray diagnostic examination is more of uncertainty. But it is important to ensure that such uncertainty in measurement are reduced if not eliminated.

2.2 Radiation dosimeters

Radiation dosimetry is basically the quantitative determination of that energy absorbed in a matter (Podgorsak, 2005).

There is no particular organ identified in man which can detect the presence radiation and has not been impossible till date for any scientific initiative to come out with any instruments that can amplify human's response to radiation, in contrast to the case of visible light wave (optics). However, there is dependence on instruments to indicate the presence of ionizing radiation (Kyere, 2018).

Radiation dosimeter helps to detect and quantify ionizing radiation. A radiation dosimeter is an instrument that measures the dose of ionizing radiation and consists of a measuring assembly: electrometer, and at least one detector assemblies which can either be a key component of the measuring assembly or not.

In conventional radiography dosimetry, reliable dosimeters such as ionization chambers or semi-conductor detectors are used in the measurement of air kerma (K), air kerma length product (P_{KL}) air kerma rate ($\dot{k}$) and air kerma area product (P_{KA}) in primary beam conditions. Measuring of dose is important when it comes to quality control and acceptance test (Okuno, 2012).

2.3 Gas filled detectors.

The most common type of instrument used to indicate the presence of ionizing radiation is a gas filled radiation detector. Figure 2.1 is a schematic diagram of s gas filled detector.

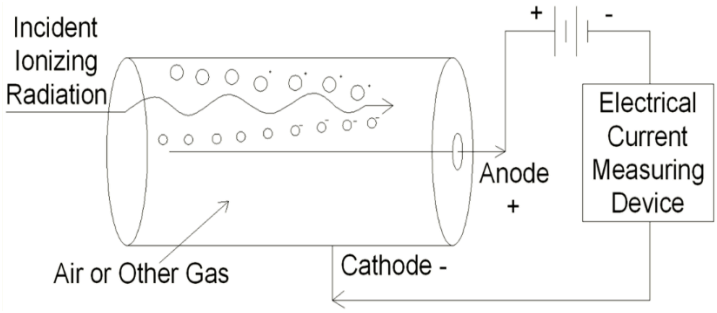

Figure 2.1 Principle of a gas- filled detectors

.

2.3.1 Principle of operation of gas filled detectors

The principle behind the operation of the gas-filled detector that when ionizing radiation is allowed to pass through air or gas, the molecules of the air or gas get ionized. The positive ions will be attracted to the negative side of the detector (the cathode) when a high voltage is imposed between two areas of the gas filled vacuum, and the free electrons will migrate to the positive side (the anode). The anode and cathode, forming a very small current in the wires going to the detector, collect these charges. The current is

measured and shown as a signal by putting a very sensitive current measuring device between the wires of the cathode and the anode. The more radiation reaches the chamber, the more current the instrument shows.

According to Ahmed (2007), the design of a gas fill detector is of three essential components: an anode, a cathode, and a gas enclosure. Most detectors use the wall of the container that holds the gas and a wire inside the container as cathode and anode respectively.

The design of gas-filled detectors and applied voltage constitute their classification as either ionization chambers, proportional counter, or Geiger- Muller counters. Figure 2.2 shows the various regions of a gas filled detector.

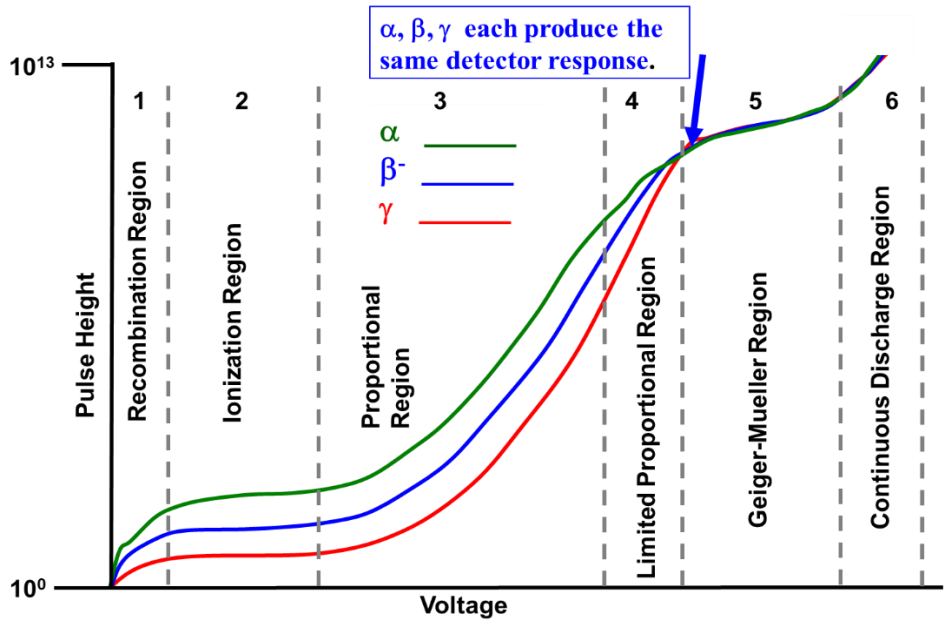

Figure 2.2: Operational regions of s gas filled detector (NET 130, 2018)

2.3.2 Characteristics of different regions across a gas-filled detector.

2.3.2.1 Recombination Region

In the recombination region, the voltage applied is low, and hence low electric field strength exist within the chamber. This leads to ion recombination since only small charges are collected from the gas. The recombination of positive and negative ions within the air cavity reduces the amount of charge collected. At this region, not all the signals produced are collected as charges due to the recombination effect (Mayles et-al., 2007).

2.3.2.2 Ionization Chamber Region

Increasing the electromotive force (EMF) accelerate more electrons from the recombination zone. The region of full ionization (i.e. the ionization chamber region) is then reached. This is also known as saturation region. At the saturation region, the applied voltage is high enough to prevent recombination and low enough to prevent secondary ionizations. The signal becomes constant over a wide voltage range. All primary ion pairs are collected on electrodes. The operating voltages of an ionization chamber can be found within a range of 500–1000 V (Knoll, 2010).

2.3.2.3 Proportional Region

Further increase of the Electromotive force (EMF) beyond ionization chamber region, forces the electrons produced in the gas to be accelerated to such an extent that they produce additional ionization of the gas. This is called the proportional region and there is increases in the charge collected on electrodes. It is called proportional region because

there is direct proportionality between number of ions pairs collected and number of ions pairs initially produced in the detector by radiation if the voltage remain constant. This means that for a given detector and particular voltage its gas amplification factor is always a constant (Mayles et-al., 2007).

2.3.2.4 Limited Proportional Region

At the proportional region, increase in the Electromotive force (EMF) results in the expansion of the ionization zone and significant gas amplification is obtained. Further increased in voltage, results in space charge effect starts to reduce the effective electric field and affects the gain. The limited proportionality region is then entered. This is not a very useful range for radiation detection. The collected charge becomes independent of the number of primary ionizations. The secondary ionization leads to photo ionization and the constant of proportionality is no longer exact (Knoll, 2010).

2.3.2.5 Geiger-Mueller (GM) Region

As the Electromotive force (EMF) is increased, beyond limited proportional zone, a point of massively multiple, successive ionizations of most of the gas within the detector is reached. No more gas amplification is possible once all the gas is involved. This implies that any further increases in voltage has little or no effect on the size of the pulse of current. The detector is said to be operating in Geiger–Müller region and hence called a Geiger–Müller counter. In the Geiger –Muller region, the size of the current pulse does not depend on any small changes in voltage, (Knoll, 2010).

2.3.2.6 Continuous Discharge Region

At the continuous discharge region, electric field intensity becomes so strong that no initial radiation event is needed to completely ionize the gas by increasing voltage beyond the Geiger-Müller zone. Secondary ionization is propagated by the electric field itself, and complete avalanching takes place. There is no feasible practical radiation detection (Knoll, 2010).

2.4 Ionization chambers

The International Electrotechnical Commission (IEC) defines ionizing radiation detector as a chamber enclosed with air, in which an electric field insufficient to produce gas multiplication is provided for the collection at the electrodes of charges associated with the ions and the electrons produced in the measuring volume of the detector by ionizing radiation (IEC 61674, 2013).

Both electrodes are separated with a high-quality insulator to reduce the leakage current when a polarizing voltage is applied to the chamber. They are in different sizes and shapes, depending on the specifications. The operation of the chamber changes as the voltage increases. Generally, they operate in the near saturation or saturation region (Okuno, 2012).

For any high-quality technical measurements, ionization radiation detector is often employed. It the most preferred choice for over a very long period. (Ross, 2009.)

It is recommended that the ionization chambers used in diagnostic radiology be vented (the air inside the vacuum interacts with the environment), making the air mass dependent on temperature, pressure and humidity conditions (Okuno, 2012).

2.4.1 Types of Ionization chambers used in diagnostic radiology

Ionization chambers used in diagnostic radiology can be grouped into two types namely free-air ionization chambers, and cavity ionization chambers:

2.4.1.1 Free-Air ionization chamber

This type of ionization chamber is called free –air chamber because principle, the walls of the chamber do not perform any role in its response. They are used to measure direct exposure now air kerma in photon beams.

The measurement involves the collection of all ions which are produced by the radiation beam as a result of direct transfer of energy from photon to primary electron in a defined volume of air. They are practically limited to photon energy below 0.3 MeV. It is practically impossible to build such a chamber for higher energies due to the increase in secondary electrons (Mayles et al., 2007).

2.4.1.2 Cavity ionization chambers

Cavity ionization chambers consist of an envelope surrounding a gas volume (air in this case) between electrodes (-polarizing and central electrode) with an applied voltage. An electric field is created when a voltage is applied to the two electrodes inside the cavity. This electric field collects the charges resulting from the ionization of the air by electron entering the cavity. The amount of incoming electrons is proportional to the radiation received.

Basically, cavity chamber are grouped into two: cylindrical (thimble) chamber and parallel plate (plane parallel). Both chambers are designed to behave as Bragg Grey

cavities in megavoltage photon and electron beam and their designs features can best be understood in the light of this theory (Mayles et al., 2007).

Cherry et al. (2012), advises that the gas cavity should be sufficiently small to prevent the disturbance of the particle fluence could result in same number and energy of electrons traversing through the volume.

Measurements of air kerma in air for energies in the ranges of 0.6 to 1.5 MeV is done by cavity ionization chambers Ions are collected in a defined volume, inside a cavity, enclosed by graphite body which is thick enough to provide full build-up of secondary electron. Cylindrical chambers are uniformly sensitive around their central geometrical axis. The chambers used for measurement in the X-ray beam have effective volume of 3 cm^3 to 6 cm^3

2.5 Parallel plate ionization chamber.

Parallel plate ionization chamber (PPIC) is also referred to as plane parallel chamber because both electrodes are parallel to each other and to the entrance window (Podgorsak, 2005). Both electrodes serve different purpose, one serving as an entry window and polarizing electrode and the other as the back wall and collecting electrode. It has a guard electrode for reduction of leakage.

In conventional diagnostic radiation dosimetry, parallel plate ionization chambers have long history. There have been a number of important designs, for the absolute determination of exposure (now air kerma), and extrapolation chambers in which one can gradually reduce the distance between the electrodes by mechanical means (Nahum and Thwaites, 2011).

In 1914, William Duane, the first American Biophysicist developed the first plane parallel chamber to overcome the wall effect and measured Villard unit which he called intensity. He defined "dose" as "intensity multiplied by time in seconds" (Almond, 2009).

Subsequent chambers are developed in relation to the original parallel plate ionization chambers, but differ in terms of composition of wall material, central electrode, and/ or chamber sensitive volume and guard thickness. Figure 2.3 presents schematic diagram of a plane-parallel ionization chamber (IAEA TRS 398).

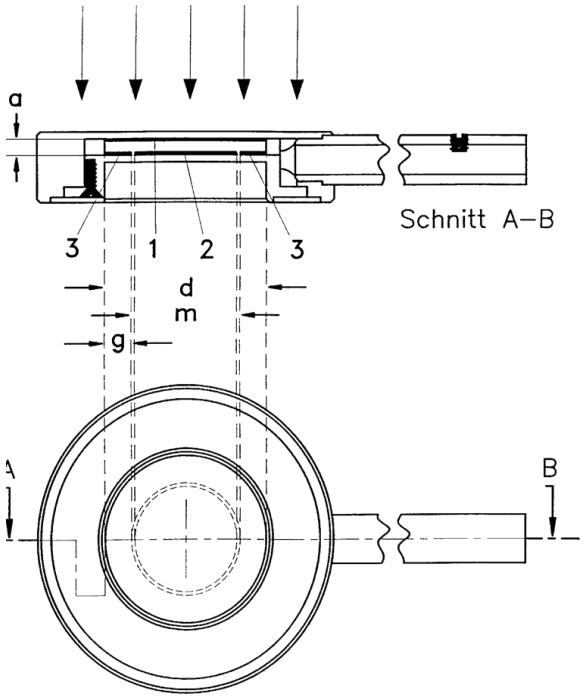

Figure 2.3 Diagram of a well-designed plane -parallel ionization chamber. Indicated in the diagram are the height a of the air cavity, the diameter d of the entrance window (1) the diameter m of the collecting electrode (2) and the width g of the guard ring (3).

Figure 2.4 is a schematic diagram of PMMA parallel-plate ionization chamber and polystyrene parallel-plate ionization chamber (Souza et al)

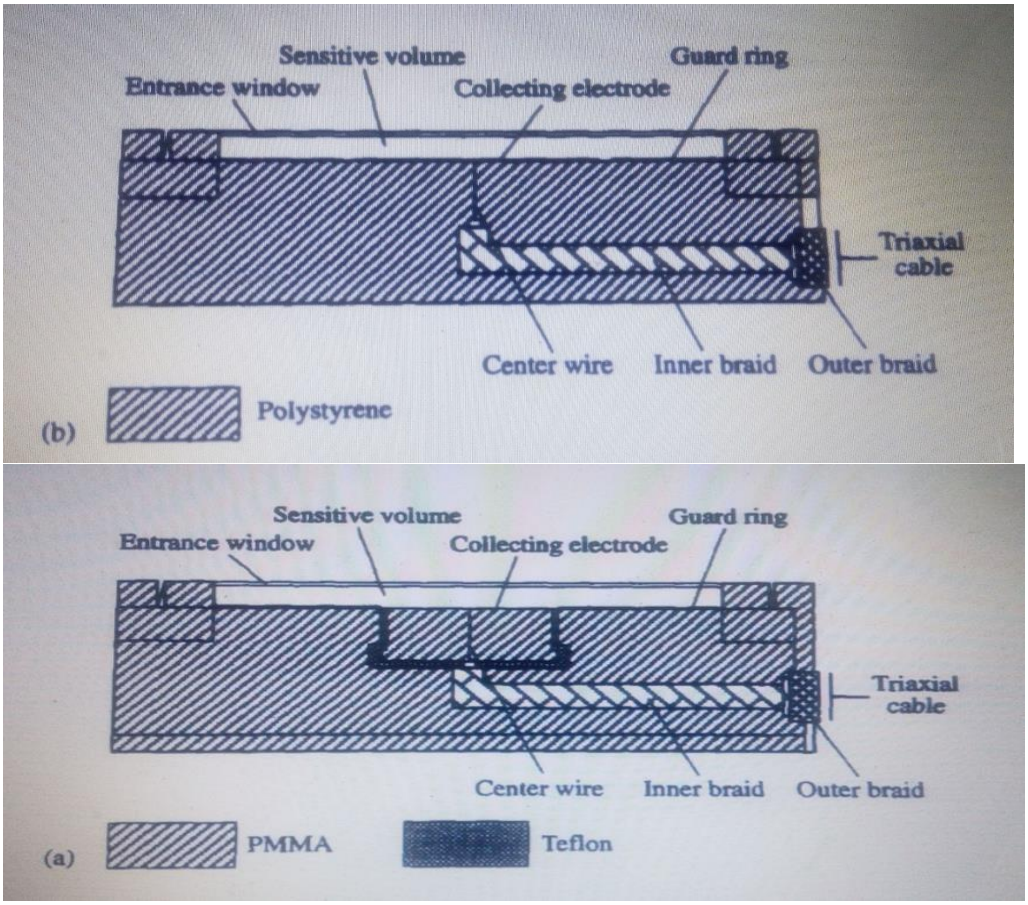

Figure 2.4: Schematic diagram of (a) PMMA parallel plate ionization chamber and (b) polystyrene parallel plate ionization chamber

Today, parallel plate ionization chamber remains the most common type of ionization chamber for diagnostic radiological measurement of air-kerma (Mayles et al., 2007).

For dosimetry of electron beams with energies below 10 MeV, and higher photon beams, plane parallel is the mostly preferred choice. Its major limitation is the angular

dependence response. It should always be placed perpendicular to the radiation beam (Dance, 2014). Schematic diagram and dimensions of standard plane-parallel chambers is presented in Figure 2.5.

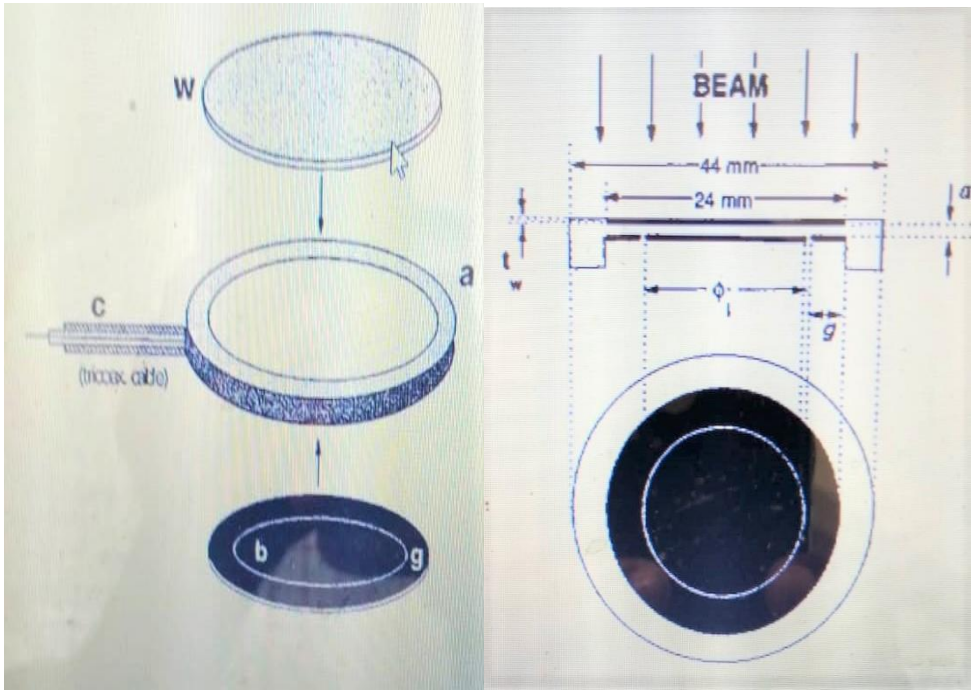

Figure 2.5 Schematic diagram and dimensions of parallel plate ionization chamber w: is the outer/ polarizing electrode, b: inner/ measuring electrode, g: guard ring, a: the height of air cavity, ∅ : the diameter of the collecting electrode. g: the width of the guard ring (Solimanian et al, 2005).

2.6 Physics of parallel plate ionization chambers

Ahmed, (2015), "explains that as radiation interact with gas, it ionizes the gas molecules, if its energy is higher than the ionization potential of the gas. By the application of an external electric field, the ion pairs created can thus be made to move in opposite

direction. The result is an electric pulse can be measured by an associated measuring device

Andreo et al, (2005), explains that, when ionizing radiation, such as x-ray is allowed to pass through the entrance window (polarized electrode) it ejects a high energy electron into the sensitive volume. The electron ionizes the air in the sensitive volume, yielding cation and low energy electrons. The electronegative oxygen attracts the low energy electron, producing negative ions. The positive electrons are attracted by polarizing electrode while negative ions goes to the measuring electrode creating a charge Q in the known sensitive volume of air and the total charge measured. If voltage applied is relatively low, the electric field E is too weak to efficiently separate the negative and positive charges. Primary and secondary ions produced within the gas are separated by Coulombic effects.

Dose in air is calculated using Bragg Gray cavity theory (Andreo et al., 2005) in equation 2.6:

$$D_{air} = \frac{Q}{m_{air}}\left(\frac{W_{air}}{e}\right) \qquad (2.6)$$

where: D_{air} is dose in air Q is ionization charge m_{air} is mass of air in the sensitive volume

$\left(\frac{W_{air}}{e}\right)$ is the mean energy required to produce an ion pair in per unit charge.

(33.97J/C $^{\pm 0.06}$ for dry air, ICRU 1984)

Dose in a medium is deduced from Bragg-Gray and Spencer-Attix cavity theory (Andreo et al., 2005), which links dose in air, dose in a medium and dose in the wall according to the following correlation

$$D_{med} = D_{wall}\left(\overline{\frac{\mu_{en}}{p}}\right)_{med,wall} = D_{gas}S_{wall,gas}\left(\overline{\frac{\mu_{en}}{p}}\right)_{med,wall} = \frac{Q}{m}\left(\frac{W_{gas}}{e}\right)S_{wall,gas}\left(\overline{\frac{\mu_{en}}{p}}\right)_{med,wall} \quad (2.7)$$

Where $S_{wall,gas}$ is the ratio of restricted mass collision stopping power for cavity wall and gas.

In practice: $$D_{med} = \frac{Q}{m}\left(\frac{W_{gas}}{e}\right)S_{wall,gas}P_{fl}P_{dis}P_{wall}P_{cel} \quad (2.8)$$

where: P_{fl} electron flounce perturbation correction factor.

P_{disl} the correction factor for displacement of effective measurement.

P_{wall} wall correction factor.

P_{cel} the correction factor for central electrode.

Podgorsak (2005), explains that, the Bragg-Gray cavity theory is applicable under the following conditions:

i. The cavity must be small when compared with the range of charge particles incident on it, so that it presence does not perturb the fluence of charge particles in the medium.

ii. The absorbed dose in the cavity is deposited solely by charge particles crossing it.

According to Seco (2014), the quantity of charge induced, dQ, by either an ion or a single electron moving a distance within an electric field, E in an ion chamber can be calculated by:

$$\frac{1}{2}V_0^2 dQ = qEdl \quad (2.9)$$

where V_0 is voltage difference across the electrodes and q is the electron or ion charge.

2.7 Components of a typical parallel plate ionization chamber.

The components of a typical parallel plate ionization chamber can be grouped into two major forms; the measuring assembly and the chamber assembly

2.7.1 Measuring Assembly

The measuring assembly for the parallel-plate ionization chamber includes an electrometer and a power supply for polarizing voltage of the ionization chamber. The electrometer should preferably be provided with a digital display and should be capable of four-digit resolution; it should allow 0.1% resolution on the reading. The variation in the response should not exceed ± 0.5% over 1 year period (i.e. long-term stability) (IAEA TRS-381). The electrometer (Figure 2.6) and ionization chamber can be calibrated separately. In centers provided with many electrometers or chambers, this is particularly useful. The electrometer is an integral part of the dosimeter in some situations, however, and the ionization chamber and the electrometer are calibrated as a single unit only. Due to the determination of polarity effect and ion collection efficiency, the electrometer polarising voltage polarities must be reversible,.

Figure 2.6 PTW Unidos Electrometer

2.7.1.1 Cables and Connectors.

Cable and connectors play a major role in dosimetry. The chamber and the electrometer are coupled together by high-quality low-noise triaxial cable and a connector. To ensure good contact and rigidity, the connectors are mostly made male and female. Some connectors may have protective covers which veil the real shape of the connector.

The cable has three conductive wires which are separated by insulators. The following are the desired cable characteristics:

i. Low capacitance.

ii. Pliability

iii. Short equilibration time (less than one minute) when the high voltage is changed

iv. Low radiation-induced signal

v. Low microphonic noise

vi. Low leakage (less than 10^{-14} A).

Basic problems uncounted by users with the connectors of the chamber cable and the electrometer includes, mismatches of connectors resulting to improper contacts, dirt, breakages in connection of the cable leading to the connector contacts, moisture, misaligned pins, strain of the cable where it meets the connector, and slightly different sizes of the same nominal connector. It is important that the two devices are from the same manufacturer and consider male and female connectors so that they easily match (Mayles, 2007).

Connectors are of various types and sizes as shown in Figure 2.7.

Figure 2.7 Types of connectors used to connect an ionization chamber to an electrometer (PTW-Freiburg user manual, 2012)

2.7.2. Chamber Assembly

The design of a plane parallel ionization chambers as shown in Figure 2.8 and Figure 2.9 are such that the entrance window faces the radiation source. According to (IAEA TRS-381). they are usually characterized by the following constructional details

- The air volume is a disc-shaped right circular cylinder, one flat face of which constitutes the entrance window. The central electrode is conducting circular disc inserted at the centre of the sensitive volume which forms the other flat face of the cylinder opposite to the entrance window and operates with positive voltage and collect negative charge. It is separated from chamber wall by an insulator of high quality to minimize leakage current once the voltage is applied across the electrodes.
- The sensitive volume is that fraction of the total air volume through which the lines of electrical force between the inner and outer electrodes pas.
- The inner and outer electrodes are mounted in a supporting block of material (the chamber body) to which the connecting cable is attached. The cable usually exits the body in a direction parallel to the entrance window.
- The sensitive volume is typically between 0.05 cm^3 and 0.5 cm^3.
- The polarizing potential is applied to the outer electrode and the signal charge is collected from the inner electrode;
- There is usually a third electrode surface between the other two which is not connected electrically to either of them, but which is designed to be held at the same potential as the inner electrode. If the chamber assembly is fully guarded

this third electrode will be present in the air volume as a ring around the inner electrode.

Plane-parallel chambers for photon radiation have the following typical dimensions:

- The entrance window thickness is 1 mm or less
- The distance between the inner and outer electrodes is 2 mm or less
- The diameter of the inner (collecting) electrode is 20 mm or less.

Figure 2.8: A picture of a complete parallel plate ionization chamber with a connector (Rosalina Instruments)

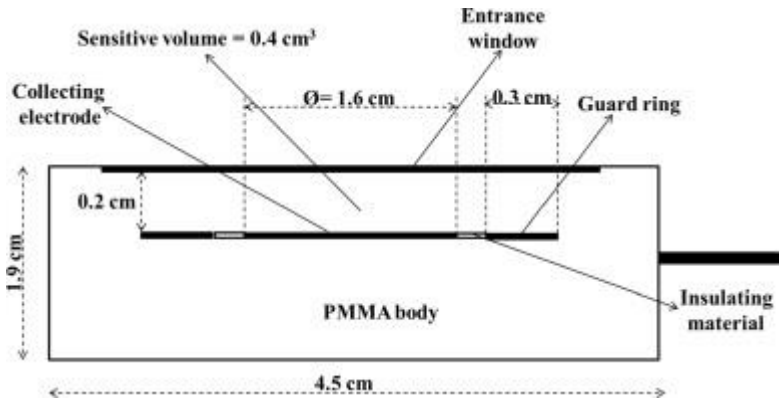

Figure 2.9: Schematic diagram of a parallel plate ionization chamber showing all the in-built components with dimensions (Chantler et al., 2014)

2.7.2.1 The Body

The body of parallel plate chambers are mostly disc shaped with diameters of Ranging from 30mm to 65mm and 10m thick.

It must be noted that, the bigger the chamber, the more sensitive it becomes

The body or shell is usually a block of non-conducting material (usually Perspex, acrylic or polystyrene).

Adequate wall thickness is necessary to give enough mechanical protection and also to achieve electronic equilibrium. However increased wall thickness result in attenuation of some photon flux, thus reducing chamber response. Contrary, decreased wall thickness than that required for equilibrium or maximum ionization, produces too few electrons in the wall, causing low chamber response as depicted in Figure 2.4 (Khan, 2010).

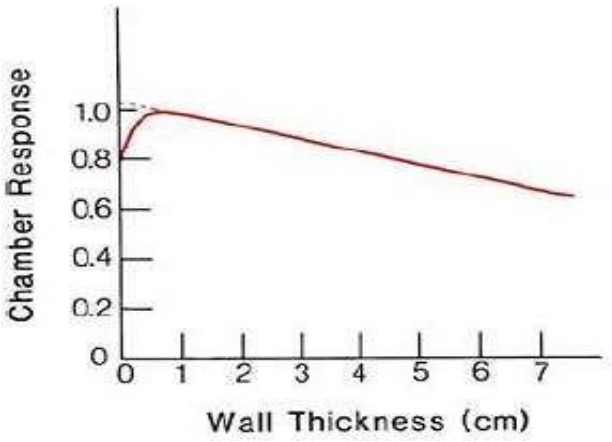

Figure 2.10 Schematic diagram of the effects of wall thickness on the chamber response (Khan)

2.7.2.2 Guard

An ionization chamber does not need a guard electrode to operate correctly, but having a guard provides wonderful benefits and performance enhancements (Hooten, 2000).

The guard electrode absorbs the leakage current and allows it to directly flow to the substrate, bypassing the collecting electrode. It guarantees field continuity in the sensitive volume of chamber, with resulting advantage in the collection of charges. (Hartmann, 2012).

Some parallel-plate ionization chambers require significant fluence perturbation correction because they are provided with an inadequate guard width. Ionization chambers designed for high-accuracy dosimetry measurements use guard materials that are nearly tissue equivalent or air equivalent in atomic composition such as plastics or graphite. Use of metals lead to enhanced photoelectric effect and pair production due to high atomic number. . Figure 2.10 presents schematic diagram of a parallel-plate ionization chamber showing major components

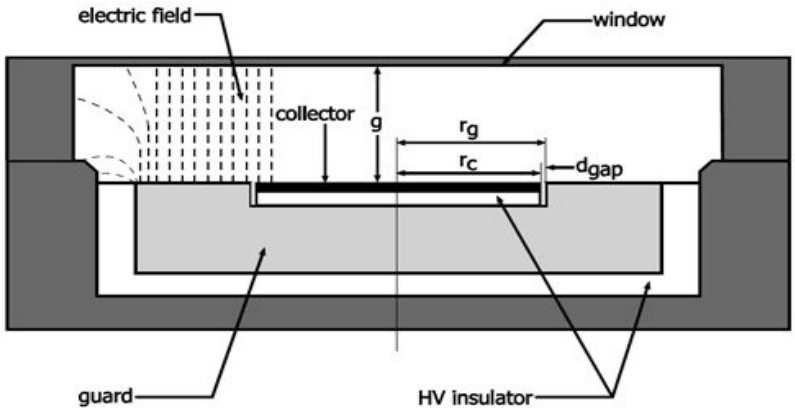

Figure 2.11 Schematic diagram of a parallel plate ionization chamber showing all the in-built components with dimension (De Ward-Ion Chambers Instrumentation)

2.7.2.3 Circuitry of a simple ionization chamber

The circuitry diagram of the parallel plate ionization chamber is shown in Figure 2.11.

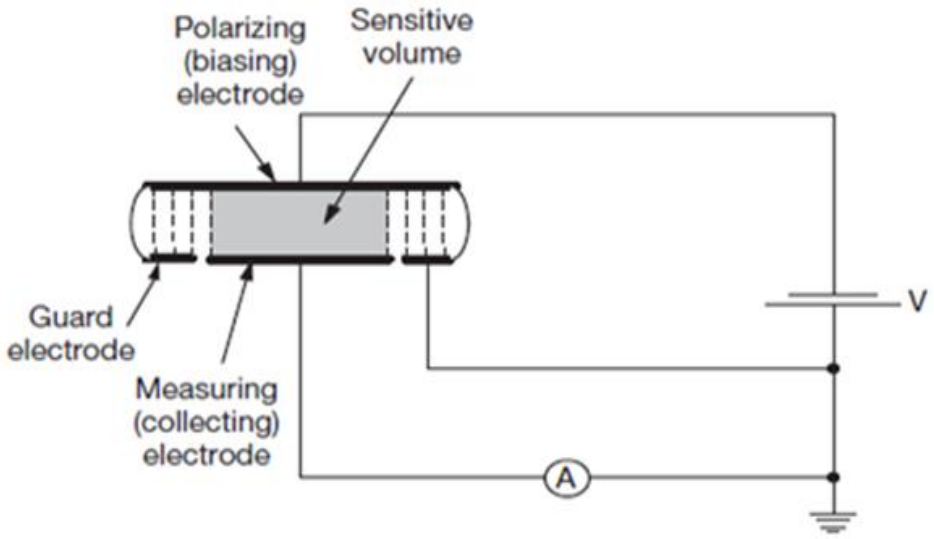

Figure 2. 12 Circuitry diagram of a parallel plate ionization chamber (Podgorsak, 2006)

The polarizing electrode is connected to the power supply directly. The measuring electrode is wired to the ground to measure the current or charge generated in the sensitive volume of the chamber via the low impedance electrometer. The Guard electrode is directly grounded and serves two purposes: it determines the sensitive volume of the chamber and prevents chamber leakage currents from being measured.

2.8 Factors Affecting the Measurement of Ionization output

Beam energy (k_e) temperature and preasure (k_{tp}) ion recombination (p_{ion}) and polarity effect (k_{pol}) are the major factor to be corrected when determining exposure now air kerma with an ionization chamber. It is expressed as:

$$\text{Exposure } (X) = MN_XK \qquad 2.11$$

$$K = k_e.k_{tp}.k_{pol}.p_{ion} \qquad 2.12$$

where X is exposure measured in C/kg, M is meter reading in C, N_X is the calibration factor of an ion chamber for standard beam energy from a national or accredited dosimetry calibration laboratory. K is a composite correction factor, K_e is the energy correction factor, K_{tp} is the correction for the air density due to the temperature and pressure, K_{pol} is correction for the polarity, and P_{ion} is the ion recombination correction factor.

2.8.1 Recombination losses

Within the ionization chamber, ion recombination losses is one of the factors that affects the current or charge measured. If the chamber is well designed and constructed, the ion

recombination effects becomes very small and are often ignored and not corrected for in X-ray systems. Such small losses are not accounted for by the user of the chamber since the calibration coefficient are also left uncorrected. (IAEA-TECDOC-1585, 2008).

If the Q1 and Q2 are the charges collected at the chamber potential of V and V/2 V, respectively, the ion recombination P_{ion} is calculated as:

$$P_{ion} = \left(\frac{4}{3} - \frac{Q1}{Q2}\right)^{-1} \qquad 2.13$$

Practically the charge Q^1 and Q are not the same.

Q^1 = Charge at low voltage, where recombination occurs.

Q = Charge at high voltage, where the chamber is saturated.

The charge Q^1 measured less than charge Q generated within the chamber due to recombination of ion pairs within the gas molecules (Atix, 1986).

According to Ross (2009), in the absence of an electric field, ion recombination will always occur. To reduce this effect, the voltage applied to the ionization chamber, must be higher enough to cause ion separation quickly to ensure that all the ions created are collected. The chamber is said to be saturated when all ions created successfully accounted for and ion recombination is totally absent.

The decrease or increase in charge is best explained by electrical design of the chamber and physics of ion transport in the chamber sensitive volume. Poor ionization geometry results in persistent recombination. For example, internal corners of chambers should be rounded not sharp.

The voltage range at which an ion chamber should be operated to achieve saturation is shown as saturation region in Figure 2.12.

Initially the curve rises linearly with increase in voltage as shown as recombination region (where ion saturation has not been achieved and complete ion collection does not take place) until a saturation is reached and finally at higher voltages it breaks down.

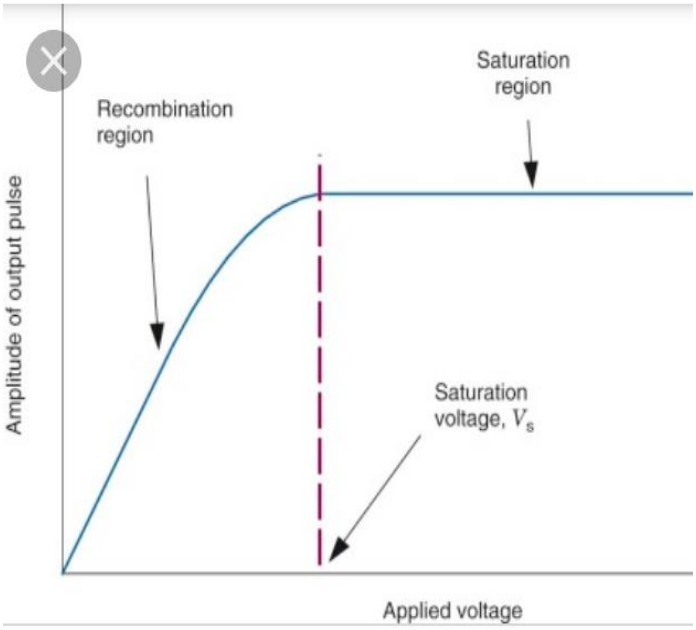

Figure 2.13: Saturation curve represents a plot of amplitude or charge against applied voltage.

Khan (2010), defines polarity effects as change in magnitude of the ionic charge collected as the polarity of the collecting voltage is reversed. Changing the polarizing potential polarities results in change in the ionization chamber current measured. This polarity effect is generally neglected especially in photon beams, but very significant in electron beams or plane parallel ionization chambers.

The correction for polarity effect, K_{pol} is calculated using equation 2.14 the following relation:

$$k_{POL} = \frac{|M^+|+|M^-|}{2M} \qquad (2.14)$$

Where, M^+ is the reading with positive polarity; $M^-$is the reading with negative polarity; and M is the polarity chosen from the saturation test. The polarity is made reference to the polarity of the bias voltage supplied to an ionization chamber. Polarity effect may be caused by extracameral current. A good example of extracameral current is current collected outside the sensitive volume of the chamber. It is caused by Compton current and irradiation of the cable connecting the chamber with the electrometer.

IEC (2013), recommends a polarity effect, K_{pol} limit of within 1.0%.

Furthermore, Khan (2010) recommends that for any radiation beam quality the variation of the chamber response between the positive and negative polarizing potential should be less than 0.5%.

Meanwhile, it is necessary to estimate the magnitude of the charge deficiency

Q – Q¹ or ion collection efficiency:

$$P_{ion} = \frac{Q^1}{Q} \qquad (2.15)$$

And make a correction to obtain a charge Q produced in the ion chamber. Where Q¹ is the measured charge by the electrometer and Q is the charge produced in the gas of the ionization chamber.

The actual measured charge, Q for the measurement of exposure, is the absolute value of mean of the two charges:

$$Q = \left| \frac{Q+ + Q-}{2} \right| \qquad (2.16)$$

The actual measured charge, Q for the measurement of exposure, is the absolute value of mean of the two charges:

$$\text{Error\%} = \left(\frac{Kpol-1}{Kpol+1}\right) \text{x100 for } Q^{--} \quad (2.17)$$

$$\text{Error \%} = \left(\frac{1-Kpol}{1+Kpol}\right) \text{ x100 for } Q^{+} \quad (2.18)$$

2.8.2 Leakage Current

Leakage current refers to any signal change recorded by the measuring assembly that is not generated by radiation (IEC, 2013).

Any current produced by the complete dosimetry system in the absence of radiation is classified as leaked current. No matter how well an ionization chamber system is designed and constructed, there is always a small amount of non-radiation, inherently exhibited due to surface and volume leakage currents which flows between the central and the polarizing electrodes of the chamber. Since, current measured by the electrometer is of the order of pico or nano amperes, any current that leaks across the insulator can greatly affects the signal output (Ross, 2009).

To prevent or reduce the effects of current leakage, guard rings or electrode is used. Use of insulators and guard electrode minimizes intrinsic current leakage. In order to ensure that no leakage of charges are induced across the inner insulator of the guard electrode, the central electrode and the guard electrode are at the same potential (TechNote4812-00, 2015). Mechanical stress like twisting and bending can induce cable leakage currents and must be avoided.

According to (IEC 61674, 2013) standard, the leakage current shall not exceed 5% of the minimum effective air kerma rate for the range in use. The indicated value shall not

change by more than 1% per minute, when a dosimeter is left in measurement mode after being exposed to the maximum effective air kerma value.

A clean insulating surface is very important and must always be maintained when constructing any ionization chamber since moisture and contaminants can reduce the resistivity of the chamber. Even the smallest microns of dust can cause large amounts of leakage.

2.9 Performance Characteristics of Parallel Plate Ionization Chamber

The IEC 61674, (2013) specifies the performance and some related constructional requirements of diagnostic dosimeters intended for the measurement of air kerma, air kerma length product or air kerma rate, in photon radiation fields used in radiography, with generating potentials not greater than 150 kV.

The complete dosimeters systems to be used for adjustment and control measurements must be of satisfactory quality and must therefore fulfil the special requirements or performance characteristics that international standard specifies. Appropriate performance characteristics should be applied to correct for any deviation from the reference conditions. Some of the corrections for influence quantities that must be accounted for in a dosimetry system include: angular dependence, energy dependence, sensitivity, linearity, and reproducibility.

2.9.1 Angular dependence

When Radiation is incident from a different angle, the detector response may vary from another different angle. This variation in response to different angle of the incidence of

the radiation source the source detector distance of 100 cm describes the angular dependence of the dosimeter (Hartmann, 2012).

The directional or angular dependence of any ionization chamber largely depends on its construction and aesthetics and the energy of the incident radiation. The angular dependence of a parallel ionization chambers might be very significant at large angle of incidence.

IEC 61674, (2013), recommends that at an incident angle of $\pm 5^{o}$, from normal 0^{o}, a response variation of ±3% upper limit is expected.

2.9.2 Energy dependence

Radiation energy determines the response of every dosimeter. In diagnostic dosimetry, the beam quality (X ray spectrum) greatly affects dosimeter readings. The quality of the beam is specified by the beam half value layer (HVL). Determination of HVL in diagnostic radiology, is a way of characterizing the hardness of the x-ray beam. Half value layer (HVL), Is the thickness of material needed to reduce intensity of an x-ray beam to one-half of its initial value, when introduced into the path of a given beam of radiation. ($I / I_o = 0.5$).

$$HVL = 0.693/ \mu \qquad (2.19)$$

HVL, usually measured in millimeters (mm) of aluminum (Al), is use to determine the effective energy. All calibrations are done at a specified beam quality, therefore it is important to correct for beam quality if the user beam quality is not the same as the calibration beam quality. The difference in response to different radiation qualities is account for by the beam quality correction factor K_Q.

For a radiation quality Q, the correction factor K_Q is the ratio of the calibration factors for quality Q to the reference radiation quality.

IEC 61674, (2013), standard recommends a ± 5% upper limit of variation of energy response in the 50 - 150 kV range while IAEA TRS 398, 2000 proposes the limit of ± 2.6 of the same ranges.

2.9.3 Sensitivity

Signal output largely depends on air kerma. The least air kerma needed to produce a signal output describe the seensitivity of a detector. A good sensitivity dosimeter, will produce a higher charge (or current) than a less sensitive dosimeter for the same air kerma (rate)

Large ionization chambers are mostly used in fluoroscopy (low air kerma rate measurements) because chambers with larger active volumes are more sensitive compared those with smaller active volumes. In radiography, where better spatial resolution is required, smaller chambers are used at higher air kerma rates.

2.9.4 Current Linearity

The linear proportionality of an ionization chamber output to the dosimetric quantities describes the linearity of the chamber. At certain range of air kerma, almost all ionization chambers exhibits current linearity, but above a certain range, non-linearity sets in, this depends on the type of chamber and it design characteristics.

It is important that all manufacturers state the dosimeter linear response range to air kerma (rate). For air kerma equation 2.21 rate must be satisfied IEC 61674, (2013)

$$\frac{Rmax-Rmin}{Rmax+Rmin} \leq 0.02 \qquad (2.20)$$

where R_{max} is the maximum response over the rated range of air kerma rate and

R_{min} is the minimum response

2.9.5 Reproducibility (Short term stability)

IEC 61674, (2013), states that the limits of variation of response when the detector assembly is irradiated in a reproducible field shall not be greater than ±2.0 % per year.

Due to the fragility of ionization chambers, any mechanical damage that may occur with little or no visible sign may result in slight changes in response of the reference chamber with time. The change is easily noticed with soft radiations unlike medium or high radiations. It is therefore recommended that stability check is done periodically to ensure that the chamber is consistent in its functions. Basically stability check of a reference chamber is achieved by either measurement in gamma beam or using stability source check like strontium-90 (90Sr). Short-term stability is evaluated by the repeatability test while long-term stability uses reproducibility test (IAEA-TECDOC-1585, 2008).

The AAPM Diagnostic X-Ray Imaging Task Group No. 6 recommends that the value obtained in each test must not differ from the reference value by more than 0.5% for short term stability. This must be determined from ten consecutive measurements made within 1hour

2.10 Ionization chamber calibration

An Accredited Dosimetry Calibration Laboratory (ADCL) is responsible for the calibration of ionization chamber in X ray and gamma beams.

To achieve high level of accuracy, precision and quality productivity, of ionization chambers, both manufacturers and users are required to calibrate the instrument. This

requires air kerma calibration factor, N_K or an absorbed dose at the radiation quality Q. If the chamber has a N_K factor, the air kerma, K_{air} at the reference depth, Z_{ref}, is given by:

$$K_{air} = M_Q N_K \tag{2.21}$$

Where M_Q is the dosimeter reading corrected for influence quantities. If the chamber is not sealed, there is need to correct M_Q for temperature and pressure as the density of air in the cavity is influenced by environmental temperature, pressure and humidity, should be applied to convert the cavity air mass to the reference conditions. The air density correction factor, K_{TP} to account for variations in temperature and pressure is given as;

$$K_{TP} = \frac{(273.15+T)P_O}{(273.15+T_O)P} \tag{2.22}$$

Where k_{TP} is the correction factor, P and T are the ambient pressure and temperature during the air kerma measurement

P_0= 101.32 kPa (1 atm) T_0= 293.2 K or 20°C are the values of the calibration reference conditions.

If the calibration coefficient was done at relative humidity 50%, there is no need to correct for humidity since it fall within 20% to 80% relative humidity.

The corrected ionization chamber response M_Q is given as:

$$M_Q = M_{raw} K_{TP} K_{dist} K_{stab} K_{others} \tag{2.23}$$

Where

M_{raw} is the mean value of the readings taken after the instrument is settled,

K_{TP} is a factor to correct for departure of air density from reference conditions,

K_{dist} is a factor to correct for the deviation of chamber position from the

reference position,

K_{stab} is a factor to correct for the stability of the SSDL reference standard,

K_{others} is a factor including all the corrections whose uncertainties are too small to consider individually in the uncertainty budget, because they are estimated to be much less than 0.1%. Nevertheless, SSDLs are advised to review and assess these factors independently to ensure that their overall contribution is indeed negligible (less than0.1%).

K_{others} is given by:

$$K_{oth}=K_{elec}K_{lin}K_{s}K_{leak}K_{h}K_{pol}K_{rot}K_{fs}K_{hom} \quad (2.24)$$

Where:

K_{elec} is the calibration coefficient of the measuring assembly, in case the chamber and measuring assembly are calibrated separately,

K_{lin} is a factor to correct for non-linearity of the measuring assembly sensitivity,

K_{s} is a factor to correct for the lack of saturation due to recombination

K_{leak} is a factor to correct for leakage current (possibly converted from an additive correction).

K_{h} is a factor to correct for any departure of humidity from the reference condition: 50% relative humidity (RH).

K_{pol} is a factor to correct for any change in the reading due to changing the polarizing voltage from its value at calibration.

K_{rot} is a factor to correct for any misalignment (rotation, tilt) of the chamber in use,

K_{fs} is a factor to correct for departure of the field size from the reference condition, and

K_{hom} is a factor to correct for radial non-homogeneity of the beam

IEC 61674 explains that sealed chambers, in which the air volume does not change, are not suitable for diagnostic radiology dosimetry; their necessary wall thickness may cause unacceptable energy dependence, while the long term stability of the chambers is not guaranteed.

2.10.1 Cross calibration

Cross calibration is a general term used to describe the direct comparison of reference instrument that has been calibrated at a secondary standard dosimetry laboratory (SSDL) and a field or newly constructed instrument in a suitable quality beam (IAEA-TRS 457, 2007).

The two methods used in cross calibration include tip-to-tip and substitution method. For the tip to tip method, both the reference ion chamber and the one to be calibrated are irradiated together and readings are recorded for each of them (IAEA-TECDOC-1585, 2008). To ensure that, scattered radiation for each of the detectors are the same, the two detectors are of a similar design. (IAEA-TRS 469, 2009).

For the substitution method, reference output rates of the beam with the reference detector are determined through a set of readings. The detector to be calibrated is put under the same conditions and similar sets of reading are taken and recorded. This method is adopted when the chambers to be compared are very different in size or shape. With the substitution method, the beam non uniformity accuracy is less compared to the tip-to-tip calibration method (IAEA-TECDOC-1585, 2008).

CHAPTER THREE

MATERIALS AND METHODS

3.1 Introduction

In this chapter, the conceptual design, materials and experimental methods are presented. The construction processes includes designing, machining, drilling, bonding and assembling of the components. The pre-evaluation tests to ensure that the ionization chamber satisfies the IEC 61674 (2013) standard has also been presented.

.3.2 Materials used

Table 3.1 presents a brief description of the major materials that were used for constructing the ionization chamber.

Table 1.1 Properties of materials used to construct the chamber

S/N	Material	Properties/Characteristics
1	Aluminium	Aluminium is a good conductor of heart and electricity with a melting point of 660 ^{O}C. It is light in weight, malleable, ductile and non-corrosive.
2.	Copper	Copper has a melting point of 1080 ^{O}C. It a good conductor of electricity and heat. Its malleable, ductile and non-corrosive
3	Polymethylmethacrylate (PMMA)	PMMA Is one of the durable materials used for the construction of ionization chamber. It is transparent and easy to machine. It is used as an electrical insulator

3.3 Equipment needed to evaluate the performance characteristics.

i. Acuity Conventional Radiotherapy Simulator

ii. PTW Unidos electrometer

iii. Digital thermometer

iv. Digital barometer

v. Piranha Diagnostic Multimeter

3.3.1 Acuity Conventional Radiotherapy Simulator

Acuity Radiation Treatment Planning Simulator (MPN: 316900714) is a KV X-ray machine and detector, that is attached to a machine that emulates the movements of a radiotherapy treatment machine as linear accelerator (LINAC). Therefore it makes it possible to produce X-ray images from the patient body under positioning conditions simulating a LINAC and make it possible to control all parameters on the treatment plan such as the field size, beam directions and collimator setting. The gantry and collimator (to shape the desired field size and direction) can rotate about angle of ±190° and ±185°, respectively, and a frame Laser positioning or alignment system (LAP Apollo).

It has exposure parameters of fluoroscopy and radiography modes, up to 150 kVp and 300 mAs (radiography) and 4 mA (fluoroscopy) with 2.5 mmAl filter and 30 kW high. It was manufactured by Varian Medical Systems in the year 2008 and the X- ray tube was changed in 2019. This Radiation Treatment Planning Simulator shown in 3.1 was used during the performance characteristic test of the newly constructed chamber.

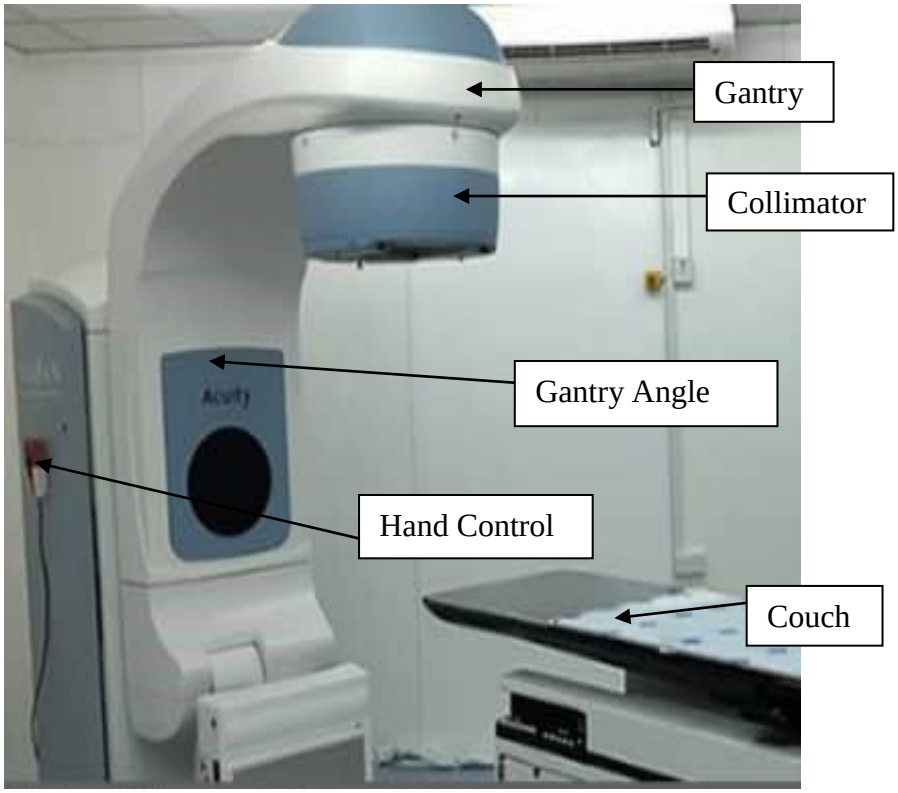

Figure 3.1: Acuity Conventional Radiotherapy Simulator

3.3.2 PTW Unidos Electrometer

The PTW Freiburg Unidos Electrometer (SN: 1053, Version: 2.40i- Germany) is used to supplies bias voltage to the ionization chamber. It can operate in radiological mode for measuring small current. It has a large liquid crystal display (LCD). It has a bias voltage of ± 0 – 400 V with 50 V increment. The polarity of the bias voltage can be selected by the use of a switch at the back of the electrometer. The electrometer was calibrated together with its accompanying ionization chamber.

When taking dosimetric measurements, the chamber was connected to the electrometer to obtain the chamber response to radiation. During measurement in this study, the

electrometer was operated in current mode, hence the measurement parameters are in pico amperes (pA). Figure 3.2 shows the PTW Freiburg Unidos Electrometer used in this study.

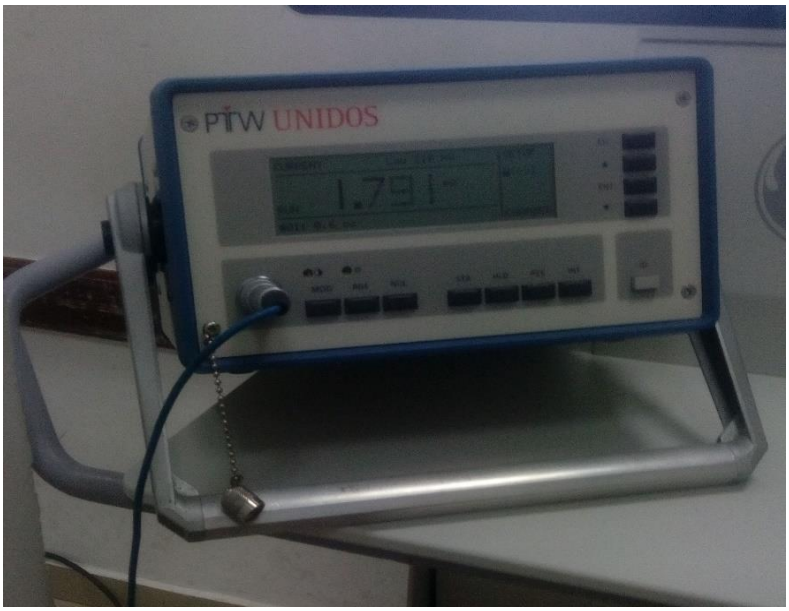

Figure 3.2 PTW Unidod Electrometer

3.3.3 Digital Thermometer

The Dostmann Electronic Digital thermometer (SN P700, Germany) with dimensions 200 mm x 93 mm x 44 mm was used during charge measurements to correct the effects of temperature differences between the standard reference temperature of (20.0 ºC) and the temperature recorded at the facility under different environmental conditions. It has a detachable measuring probe that is fixed into position before it can be used. Figure 3.3 shows the thermometer that was used in this study. It measures-temperature

in ^{O}C – Celsius and ^{O}F - Fahrenheit with allowable operating temperature of 0 °C to +40 °C and highest accuracy degree of ±0.03 °C

Figure 3.3 Digital Thermometer

3.3.4 Digital Barometer

A hand held Digital Barometer (Model: XA1000, Germany) for barometric air pressure 800 - 1100 mbar with dimensions 170 mm x 62 mm x 34 mm was used during current measurements to correct the effects of pressure differences that may exist between standard reference pressure (101.325 hPa) and pressure recorded at the study centre. It is simple operated by touchscreen and has ±0.5 mbar degree of accuracy. It is used for accurate measurement of the barometric air pressure up to 4000 m latitude above sea

level. Figure 3.4 shows the barometer that was used. It has external sensor for climate measurement application for temperature, humidity and air flow.

Figure 3.4 Digital Barometer

3.3.5 Piranha Diagnostic Multimeter

Piranha Diagnostic Multimeter (SN: CB2-15020088, RTI-Sweden) is used for quick quality control (QC) test in radiography, fluoroscopy, computed tomography (CT), dental, and mammography. The unique features of the Piranha Diagnostic Multimeter makes it possible to check the position (position check) of the detector before measuring.

This verifies that the detector area is fully irradiated. It is a solid-state detector and hence no need to compensate for temperature and pressure. Its compatibility with the Ocean diagnostic software and provides quick and repeatable Quality Control (QC) activities. It measures and presents all parameters instantly and simultaneously. Figure 3.5 shows the Piranha multi that was used to validate the newly constructed chamber.

Figure 3.5: Piranha multimeter

3.4 Conceptual Design

The conceptual design of the parallel plate ionisation chamber was developed and evaluated. This concept of a portable parallel plate ionization chamber design comprises of an entrance window which is mechanically secured on top of the main body by means of a screw. The bias electrode is positioned in a way to reduce current leakage. The triaxial cable support is firmly secured into the body by means of glue. It has cork at the end to hold the cable firmly into position. Due to proximity of the measuring and the polarized electrode, recombination was anticipated to be greatly reduced. With this

design, effective functioning of the ionization chamber was expected. Figure 3.6 and 3.7 shows sketches of the design concept.

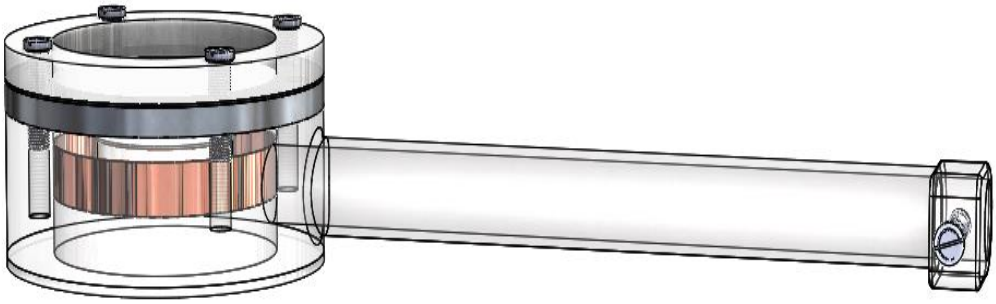

Figure 3.6 Conceptual design

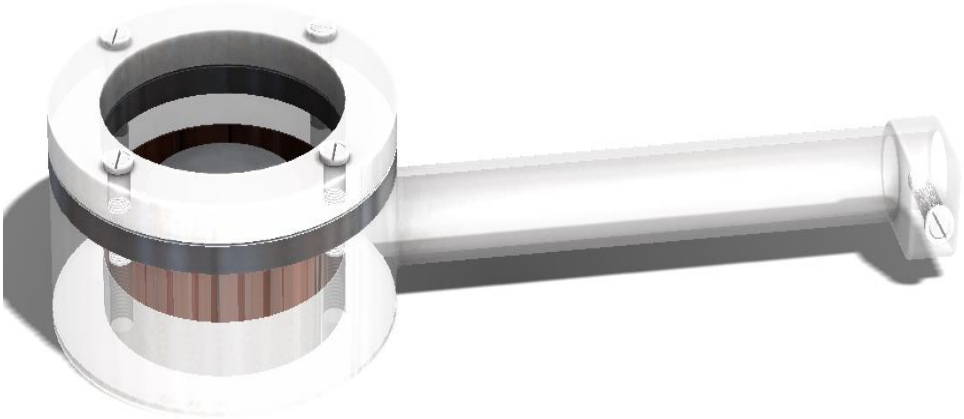

Figure 3.7 Material equivalent of the conceptual design

Figure 3.8 shows the exploded solid computer aided design (CAD) model of the parallel plate ionization chamber in stepwise arrangement of the components.

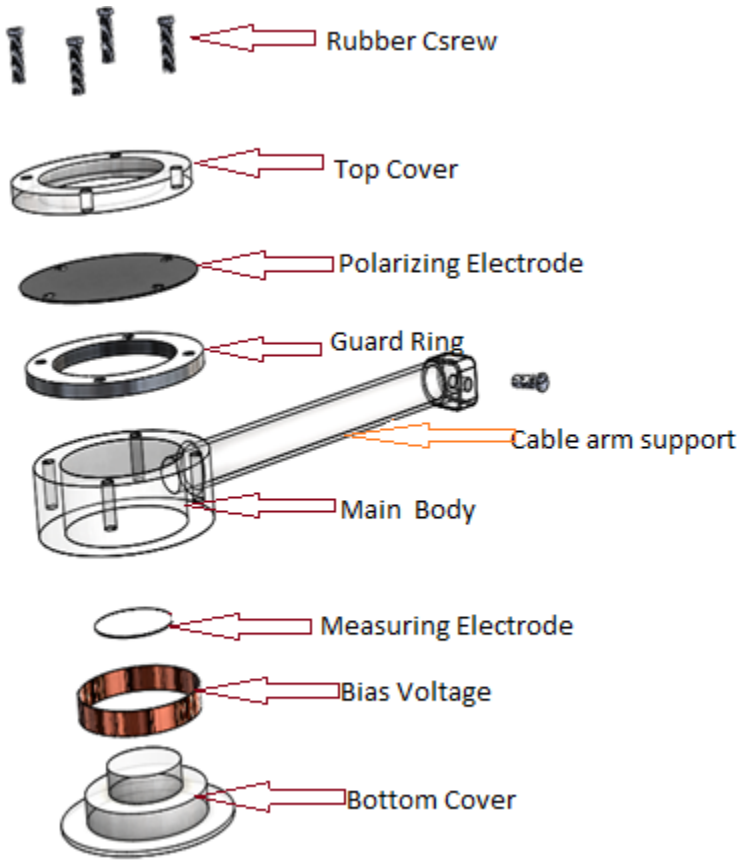

Figure 3.8 Exploded solid CAD model of the parallel plate ionization chamber

3.5 Assembling processes

The bias electrode was first fixed onto the bottom cover. The measuring electrode was fixed on top of the bottom cover. These three components were securely fixed into the body. The top cover, polarizing electrode and the guard ring are all aligned into position to take the screws. The crews are further tightened to ensure firmness. The various components were assembled by using adhesive and screws.

Figure 3.9 Assembled components

Figure 3.10: Assembled parallel plate ionization chamber

3.6 Evaluation of constructed Parallel plate ionization chamber performance characteristics

To satisfy international standards as stipulated in BS EN 61674 2013, the following dosimetric measurements were carried out to evaluate the performance characteristics of the constructed parallel plate ionization chamber.

i. Bias voltage response.
ii. Angular /Directional dependence
iii. Pre- irradiation current leakage
iv. Current Linearity
v. Half value layer (HVL)
vi. Short term stability (Consistency)
vii. Repeatability
viii. Chamber calibration.

These performance characteristics test were carried out at National Radiotherapy Oncology and Nuclear Medicine Centre at the Korle – Bu Teaching Hospital (KBTH) Accra, Ghana.

3.6.1 Chamber response to Bias voltage

The bias voltage was determined by selecting various voltages from the electrometer and irradiating the chamber, while corresponding readings were recorded. An open field of 10 × 10 cm^2, 100 cm SSD technique was adopted. The chamber's voltage ranged between -400 V to +400 V with 50 V incremental intervals. The ion collection efficiency, polarity effect and saturation factor were all determined by the bias voltage response.

Effective polarity effect = (1- mean K_{pol}) ×100% (3.1)

Where K_{pol} = polarity factor

The bias voltage results are presented in Table 4.2.

3.6.2 Angular/Directional dependence

The angular dependence check was carried out using the Acuity simulation machine. An open field of 10 × 10 cm^2, 100 cm SSD technique was adopted. With increments of 10^o the gantry was moved from 0^o to 90^o anticlockwise and clockwise, while the various responses were recorded for each angle. Figure 3.11 shows the angular dependency set up. Results for angular dependence is presented in Appendix 2, Table2.B.

Figure 3.11: Set- up for the determination of angular dependency of the constructed chamber.

3.6.3 Pre-irradiation current leakage

Prior to pre-irradiation current leakage test, the electrometer was first switched on for a period of five minutes as readings were monitored and recorded without the constructed chamber connected. The constructed chamber was later connected to the electrometer and then switched on while leakage current was monitored and recorded at integral time of 100 sec. In this case, the chamber was not exposed to any radiation. Results for pre-irradiation current leakage is presented in Appendix 2 Table 2B.

3.6.4 Current Linearity test

In the current linearity test, an open field of 10 × 10 cm^2 at 100 cm SSD technique was used. The electrometer was set to a bias voltage of +300 V. The various current responses were monitored and recorded for each kVp starting from 50 kVp to 130 kVp. The chamber responses were plotted against the kVp. Results for current leakage test is presented in Appendix 2, Table 2E.

3.6.6 Energy dependence (Half Value Layer- HVL)

A narrow field size of 4 × 4 cm^2, 100 cm SSD technique was used for assessing the energy dependence. The beam was collimated to match the sensitive area of the detector to minimize scattering. The electrometer was set to a bias voltage of +300 V. Figure 3.12 shows the set up for energy dependence. Ten (10) pieces of alumunium plate measuring 50 mm x 50 mm x 1.47 mm were used during the measurements. The set up shows the angular dependency set up

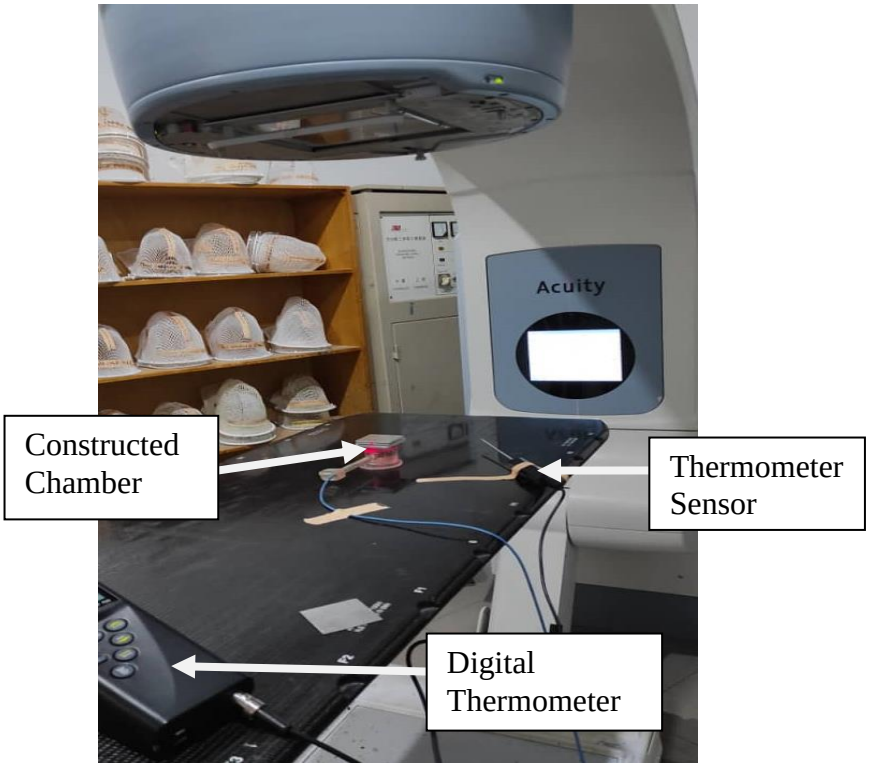

Figure 3.12 Set -up for the determination of HVL of the constructed ion chamber

First, measurement was taken without the aluminium plate and recorded. In an order of one, two, three, four etc, the plates were placed on top of the chamber until half of the measured value (output) obtained without plate is obtained. A graph of chamber response (pA) was plotted against thickness of the aluminium plates in (mmAl). The graph is presented in Figure 4.7, 4.8, 4.9, 4.10 and 4.11

3.6.7 Short term stability test

An open field of 10 × 10 cm^2, 100 cm SSD, 80 kVp, 200 ms and 20 mAs technique was used. The electrometer was set to a bias voltage of +300 V. The responses were monitored and recorded, as the same kVp was repeated ten times. A graph of chamber responses was plotted against kVp (Figure 4.2)

3.6.8 Medium term stability

Repeatability test was performed at an open field of 10 ×10 cm^2, 100 cm SSD, 80 kVp, 200 ms and 20 mAs technique. The electrometer was set to a bias voltage of +300 V. The various current responses were monitored and recorded as the same kVp was repeated in a week interval for three weeks. For all measurements, the laiser positioning alignment was used to achieve the same set up. The chamber responses was plotted against the kVp. Results for the repeatability test is presented in Figure 4.3.

3.6.9 Chamber calibration

A Piranha Multimeter with Serial number CN2-15020088 was used to cross calibrate the newly constructed chamber. Substitution method was used for the cross calibration. Measurements were taken in an open field size of 10 × 10 cm^2 at 100 SSD irradiating technique. The Piranha multimeter was irradiated from 50 kVp to 130 kVp and their corresponding exposure and exposure rates were recorded. In the same set up, the developed chamber was irradiated from 50 kVp to 130 kVp while the electrometer reading were recorded. The readings were corrected for the influences of pressure, temperature, polarity and ion recombination. Exposure in mGy recorded from the piranha was plotted against the charges in pA recorded from the electrometer to determine the calibration factor using the equation 2.11. The figure below shows the quality control set up

Figure 3.13: Set -up for the determination of QC on the Acuity simulation planning machine.

In the same set up, the developed chamber was irradiated from 50KVp - 130KVp while the electrometer reading were recorded. The readings were corrected for the influences of pressure, temperature, polarity and ion recombination. Exposure in mGy recorded from the Piranha was plotted against the charges in pA recorded from the electrometer to determine the calibration factor using the equation 2.11.

CHAPTER FOUR

RESULTS AND DISCUSSIONS

4.1 Introduction

The methodology technique use for the construction of the parallel plate ionization chamber is validated for dosimetry in X-ray systems. It discusses and evaluates the results of the construction and the findings of the performance characteristics of the developed chamber.

4.2 Characteristics of the constructed ionization chamber

The chamber was designed based on the specifications of cavity ionization chambers.

It comprises of a body made of Perspex (1.7 mg/cm^2), a bias electrode made of copper plate, a measuring electrode made of an aluminum plate, guard rings made of an aluminum plate, an entrance window made of a paper coated with a pencil (graphite), a sensitive volume of air 2.8 cm^3, triaxle cable, and a connector. The polarization voltage ranges from 200V – 400 V.

The specifications compare favourably with the standards except that the measuring electrode diameter is a little above the recommended 20 mm due to systematic error on the machine used. Table 4.1 shows the chamber characteristics and what has been recommended by Andreo et al (2005).

Table 4.1 Characteristic of the constructed parallel plate ionization chamber

C0MPONENTS	**RECOMMENDED MEASUREMENT**	**USED MEASUREMENT**
Body/Shell Ø(mm)	30 -75mm	49mm
Entrance window t_w (mm)	≤ 1mm	0.3 mm
Collecting electrode Ø(mm)	≤ 20mm	21mm
Sensitive Volume (cm^3)	0.05 – 3.5cm^3	2.8cm^3
Electrodes separation	≤ 2	1.5
Guard electrode width	7mm	5mm
Cable	Triaxial	Triaxial

4.3 Preliminary test of the parallel plate ionization chamber

4.3.1 Bias voltage of the chamber

Table 4.2 shows the response of the newly constructed chamber response with bias voltage. The responses were corrected for temperature and pressure, (K_{TP}), and polarity, (Kpol), using equations: (2.21), and (2.14), respectively. Equation 2.23 was used to calculate the corrected chamber responses (M_{corr}).

Table 4.2 Chamber response with bias voltages

(V)	$M_{(uncorr)}$	K_{TP}	K_{pol}	M_{corr}
50	91.724	1.018	0.804	75.165
100	105.414	1.018	0.891	96.741
150	108.607	1.020	0.937	98.814
200	110.545	1.020	0.971	109.552
250	110.921	1.018	0.984	111.214
300	112.634	1.019	1.002	115.082
350	112.351	1.018	0.995	114.232
400	113.924	1.018	0.997	115.741
-50	89.447	1.018	0.800	72.910
-100	98.546	1.018	0.887	86.192
-150	102.523	1.018	0.933	97.524
-200	108.295	1.019	0.968	106.821
-250	110.712	1.019	0.979	110.631
-300	113. 171	1.019	0.997	114.910
-350	111.302	1.019	0.988	112.145
-400	110.713	1.019	0.992	108.627

The corrected chamber responses (M_{corr}) were used to determine polarity effect (K_{pol}), ion collection efficiency (f_{ion}), ion recombination and saturation curve.

4.3.1.1 Polarity effect

The polarity effects listed in Table 4.3 was determined based on the polarity correction factors. Equation 2.14 was used to calculate the polarity effect of the constructed chamber. The mean value of the polarity correction factor was determined, then subtracted from unity, which is the ideal polarity correction factor. The result was then expressed as a percentage using the equation 3.1.

The mean value of the polarity correction factor was 0.97275 which resulted in a polarity effect of 2.7 ±0.03%. (M^+ Positive bias reading and $^{M-}$ negative bias reading).

Table 4.3: Polarity correction factors for various bias voltages

(kVp)	**M+**	**M-**	**Kpol**
50	91.745	89.452	0.979
100	105.452	95.332	0.901
150	108.641	102.542	0.948
200	110.563	108.281	0.971
250	110.908	110.712	0.991
300	112.625	113. 145	1.004
350	112.374	111.365	0.995
400	113.932	110.706	0.993

The polarity effect of the chamber was found to be above tolerance limit of ±1% as

recommended by IEC 61674, (2013). The effect of this is that, all the ion created are collected. This can be mitigated by re-designing of the electrodes

4.3.1.2 Ion collection efficiency and recombination

The constructed chamber ion collection efficiency (f_{ion}) response with bias voltage (V) are shown in Table 4.4. Equation 2.15 was used to estimate ion collection efficiency. The inverse of the efficiency is the saturation value (K_{sat}).

Table 4.4: Ion collection efficiency for the constructed ionization chamber

V	**M_+**	**f_{ion}**	**K_{sat}**
50	91.70	0.81	1.21
100	105.40	0.93	1.07
150	108.60	0.96	1.04
200	110.50	0.98	1.02
250	110.90	0.98	1.09
300	112.60	1.00	1.00
350	112.30	0.99	1.01
400	113.90	1.01	1.00

IAEA-TECDOC-1585 explains that for conventional diagnostic and mammographic ionization chambers, the air kerma rate and air kerma per pulse values at which the ion collection efficiency of the ionization chamber falls to 95 % when the normal polarizing voltage is applied. Andreo *et al*, 2005, explains that Ionization chamber operated at near-saturation region where the ion collection efficiency is greater than 0.97.From the table, recombination was prominent from 50 –150 V, hence saturation voltage was 200 V.

4.3.1.3 Saturation curve

Graphs of corrected chamber responses against bias voltages were plotted in order to establish the saturation voltages of the chamber, for positive and negative bias voltages as seen in Figure 4.1. The curves were a good representation of a typical saturation curve shown in Figure 2.12.

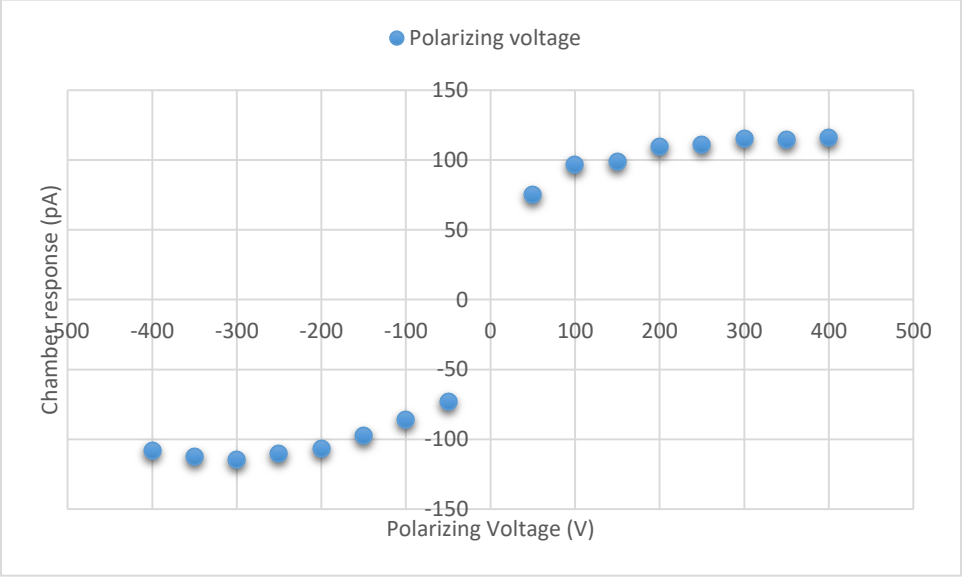

Figure 4.1: Saturation curve of the constructed ionization chamber responses

To determine the positive bias voltage equation 2.16 was used. At 350 V, the saturation factor was found to be high. The graphs were found to saturate at +200 V for positive bias voltage and -250 V for the negative bias voltage. At this linear range, change in voltage in the operational region does not have much effect on the chamber output This means that the newly constructed ionization chamber would have 99% ion collection efficiency if the maximum electrometer bias voltage was +350 V. The effects of ion recombination and charge multiplication would essentially be negligible as a result no saturation correction factor would be needed if the electrometer was operating at +350 V.

4.3.2 Stability check

4.3.2.1 Short term stability

Figure 4.2 shows a short term stability graph of normalized chamber responses against time in (seconds). The purpose is this measurement was to check for reproducibility of 10 times integral repeated response. Appendix 2: Table 2B: shows the raw data for the chamber reproducibility.

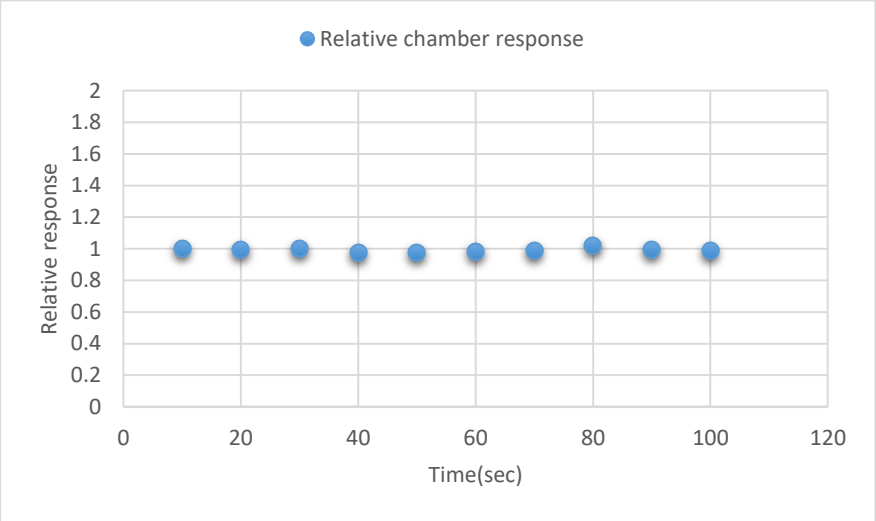

Figure 4.2: Chamber short term reproducibility response

IEC 61674. (2013), recommends ±0.5% tolerance. With standard deviation of 0.4%, the short term stability check was within the limit stated.

4.3.2.2 Medium term stability

Table 4.5 shows the weekly consistency result. To establish consistency, weekly corrected response was plotted against percentage deviation test for medium term stability,

Table 4.5: Weekly corrected response

Date	M_{corr}	% Deviation
25/09/2020	117.9	0.0
2/10/2020	112.9	2.5
9/10/2020	113.9	2

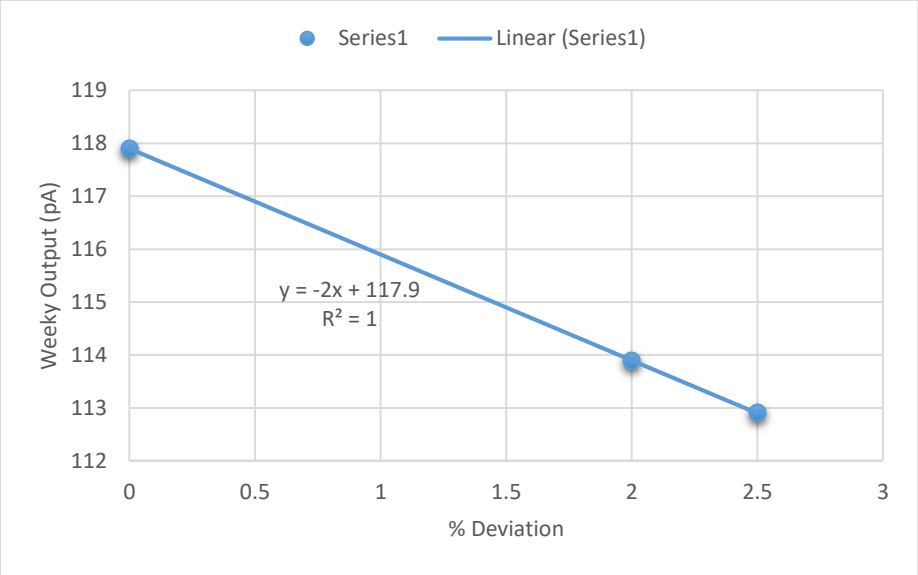

Figure 4.3 Weekly percentage deviation for medium stability (consistency) check

A graph of weekly output measured charges against percentage deviation is show in figure 4.3. The results for medium stability showed that the mean weekly deviation percentage for measured charges was 1.3% which is 0.3% above the IEC 61674 (2013), ±1.0% as recommended. This as a result of the small sample number used due to time constraints.

4.3.3 Pre-irradiation leakage current

The raw data for chamber response before irradiation is presented in Appendix 2, Table 2J. Figure 4.4 shows a graphical presentation of pre-irradiation leakage current. On the curve are displayed correlation equation, y and regression (R^2) for the dotted line of best fit to chamber responses for pre-irradiation leakage current.

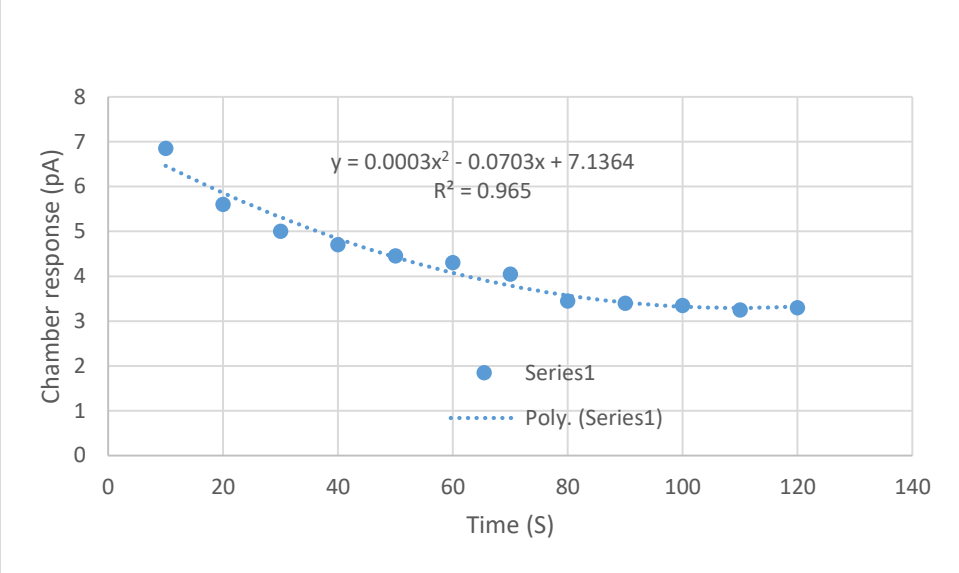

Figure 4.4: Pre- irradiation leakage test.

The results shows that initial stray charges are collected and with time their magnitude reduces.

The ionization chamber required a minimum of 2 minutes to stabilize. The maximum leakage current was 3.35pA.

4.3.4 Angular dependency

A graph of normalized chamber responses to 0^0 gantry angle response against the gantry angles is given in Figure 4.5.

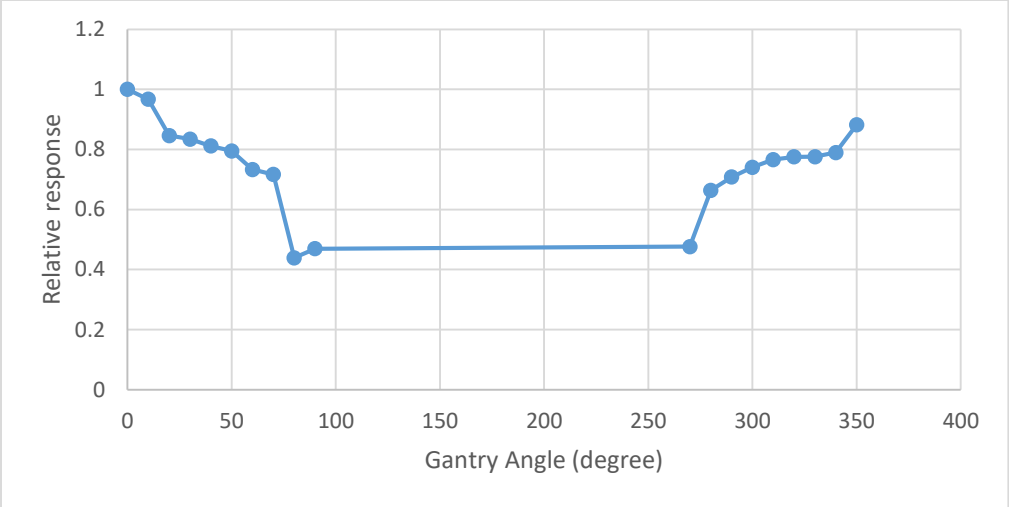

Figure 4.5: Normalized chamber response to gantry angle

The IEC 61674. (2013), standard recommends ±3% variation of response at incident angles of ±5^{o} from 0^{o}. The chamber 2.99% recorded was within the recommended range. A maximum deviation of 8.6% was observed at 90^{O} clockwise of the gantry angle. This was as a result of position of the chamber cable support and the cable its self being irradiated. Furthermore clockwise measurements had a mean deviation of 6.2%while the anticlockwise was 5.1%. It is therefore clear that the clockwise gantry movement deviated 1.1% more than the anticlockwise gantry movement due to the position of the cable support and the cable its self being irradiated.

4.3.5 Chamber response linearity

Appendix 2, Table 2E shows corrected chamber response to energy. A graphical representation of the chamber response to energy is shown in figure 4.6. A line of best fit to the chamber responses to dose represented by dotted line was drawn on each graph. A

correlation equations, y and regressions (R^2) for the lines of best fit to chamber responses are show

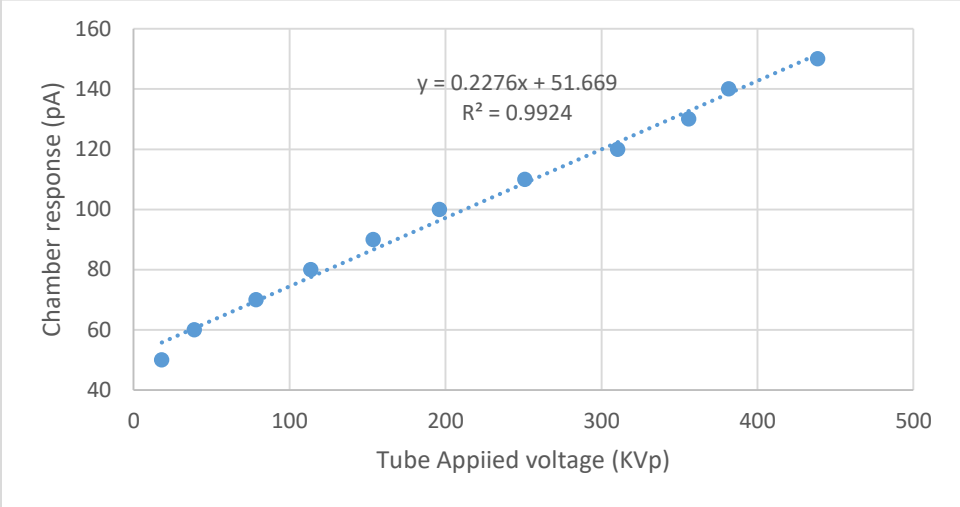

Figure 4.6: A graph of chamber response to voltages

The chamber responses to voltages were linear with a coefficient of correlation and R^2 equivalent to 0.9924.

4.3.6 Energy dependence

The constructed ionization chamber energy dependence was evaluated by plotting a graph of normalized HVL values of both detector and chamber against voltage as shown in Figure 4.7. The normalized HVL of the detector and chamber responses to various voltages are shown in the Table 4.6 below

Table 4.6: Normalized HVL responses.

kVp	Normalized Detector Values	Normalized Chamber Values
60	1.0	1.0
80	1.3	2.5
100	1.4	6.0
120	1.8	7.9
130	1.9	8.5

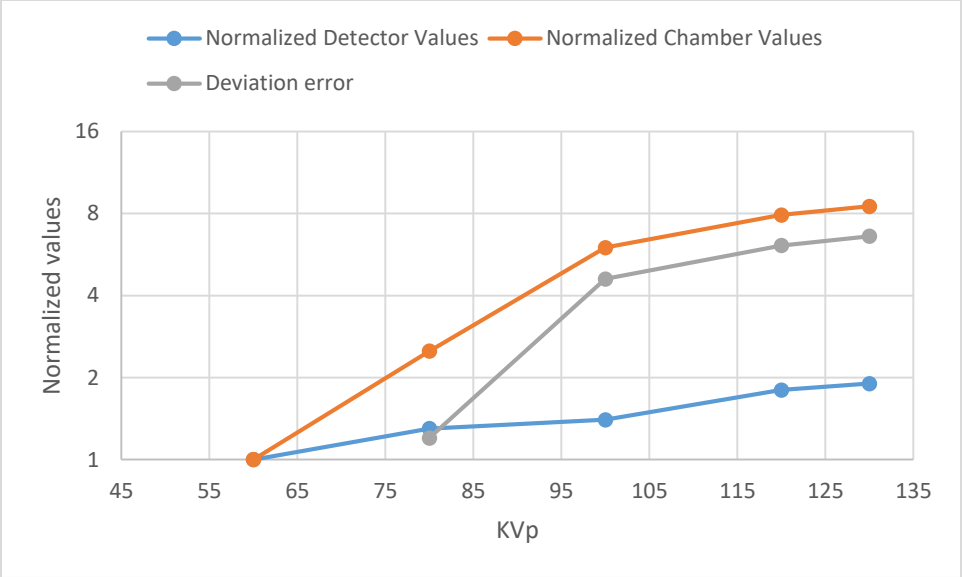

Figure 4.7: Trend of chamber HVL against detector HVL

From the graph, deviation error decrease as kVp increases and becomes stable from 100 kVp upwards. This means that at low kVp deviation error is high and diminishes at 100 kVp. It can be seen from the graph that, above 100 kVp the chamber does not depend on energy.

4.3.7 Chamber HVL Measurements

The result of HVL measurement for 60 kVp using aluminum attenuator of size 50 mm x 50 mm x 1.47 mm as shown in Table 4.7.

Table 4.7: Chamber response to Aluminium (Al) attenuator at 60 kVp

kVp	Thickness (mmAl)	Chamber response(pA)
60	0.00	38.91
60	1.47	37.24
60	2.94	31.53
60	4.41	19.55
60	5.88	9.74

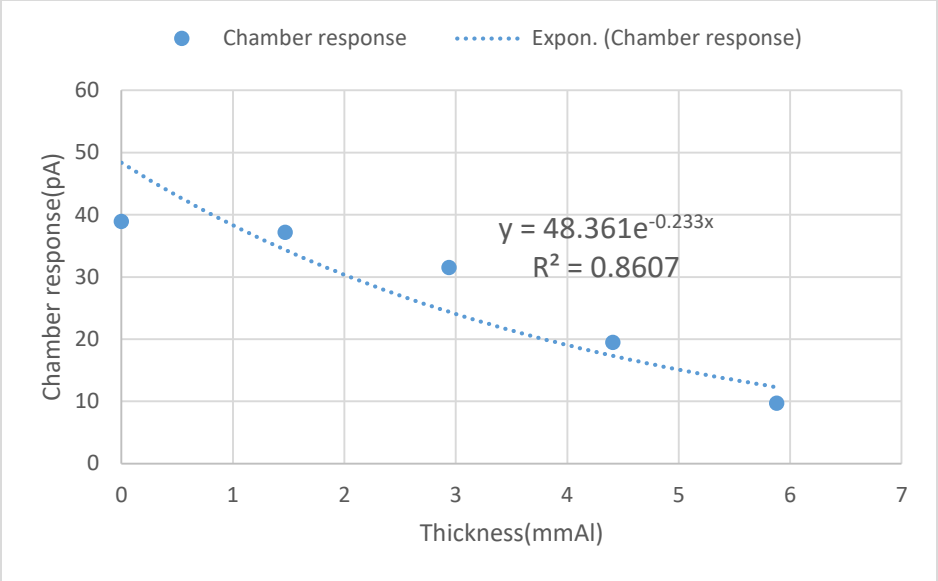

Figure 4.8: Chamber HVL responses at 60 kVp

From Table 4.7 and Figure 4.8, it can be concluded that at 60 kVp, the intensity of the beam decreases as the thickness increases till all the beams generated are attenuated. It can be concluded that an alumimium of 3.91 mm thick was used to attenuate the beam to half. .Therefore the HVL of the beam at 60 kVp is 3.91 mmAl.

Table 4.8: Chamber response to Aluminium (Al) attenuator at 80 kVp

kVp	Thickness (mmAl)	Chamber response (pA)
80	0.00	113.64
80	1.47	91.06
80	2.94	77.42
80	4.41	74.15
80	5.88	49.39
80	7.35	45.74

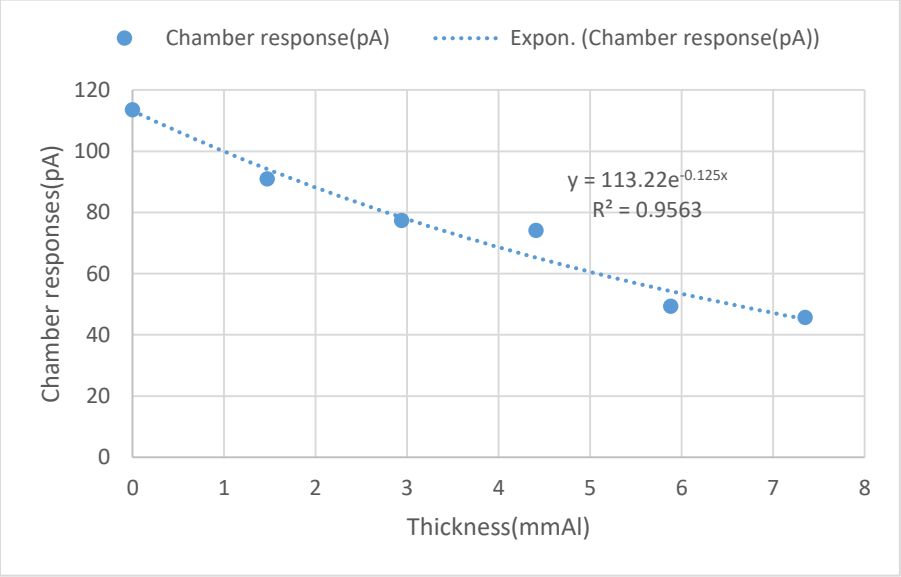

Figure 4.9: Chamber HVL response at 80 kVp

From Table 4.8 and Figure 4.9, it can be concluded that at 80 kVp, the intensity of the

beam decreases as the thickness increases till a point where all the beam are attenuated. It can be concluded that an aluminium of 5.52 mm thick was used to attenuate the beam to half. .Therefore the HVL of a beam at 80kVp is 5.52mmAl.

Table 4.9: Chamber response to Aluminium (Al) attenuator at 100kVp

kVp	Thickness(mmAl)	Chamber response(pA)
80	0.00	196.17
80	1.47	167.65
80	2.94	153.49
80	4.41	130.24
80	5.88	117.51
80	7.35	105.97
80	8.82	91.75

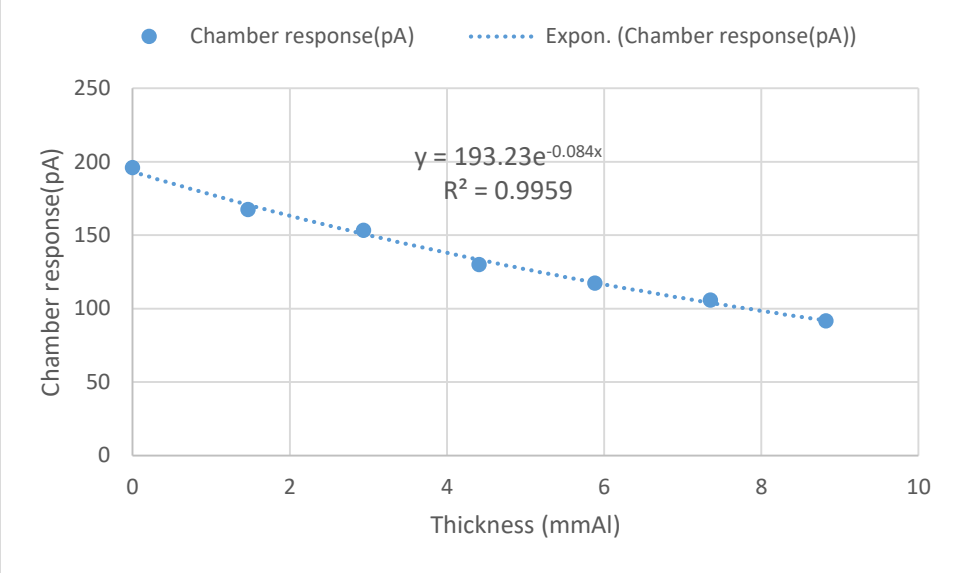

Figure 4.10: Chamber HVL response at 100 kVp

From Table 4.9 and Figure 4.10, it can be concluded that at 80kVp, the intensity of the beam decreases as the thickness increases till a point where all the beams generated are attenuated. It can be concluded that an aluminium of 8.50mm thick was used to attenuate the beam to half. .Therefore the HVL of a beam at 100 kVp is 8.50 mmAl.

Table 4.10: Chamber response to Aluminium (Al) attenuator at 120 kVp

KVp	Thickness(mmAl)	Chamber response(pA)
120	0.00	310.36
120	1.47	283.43
120	2.94	274.38
120	4.41	234.44
120	5.88	218.72
120	7.35	197.46
120	8.82	150.16
120	10.29	135.53

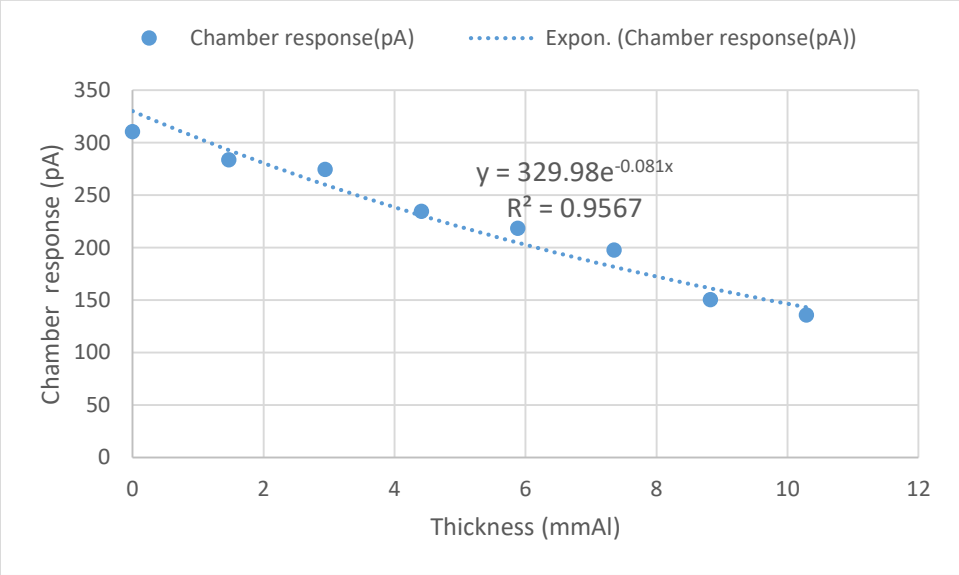

Figure 4.11: Chamber HVL response at 120 kVp.

From Table 4.10 and Figure 4.11, it can be concluded that at 120 kVp, the intensity of the beam decreases as the thickness increases till a point where all the beam will be attenuated. It can be concluded that an aluminium of 9.32 mm thick was used to attenuate the beam to half. .Therefore the HVL of a beam at 120 kVp is 9.32 mmAl.

Table 4.11: Chamber response to Aluminium (Al) attenuator at 130 kVp

kVp	Thickness(mmAl)	Chamber response(pA)
130	0.00	335.92
130	1.47	306.35
130	2.94	297.73
130	4.41	264.54
130	5.88	243.56
130	7.35	224.52
130	8.82	207.57
130	10.29	166.48
130	11.76	160.44

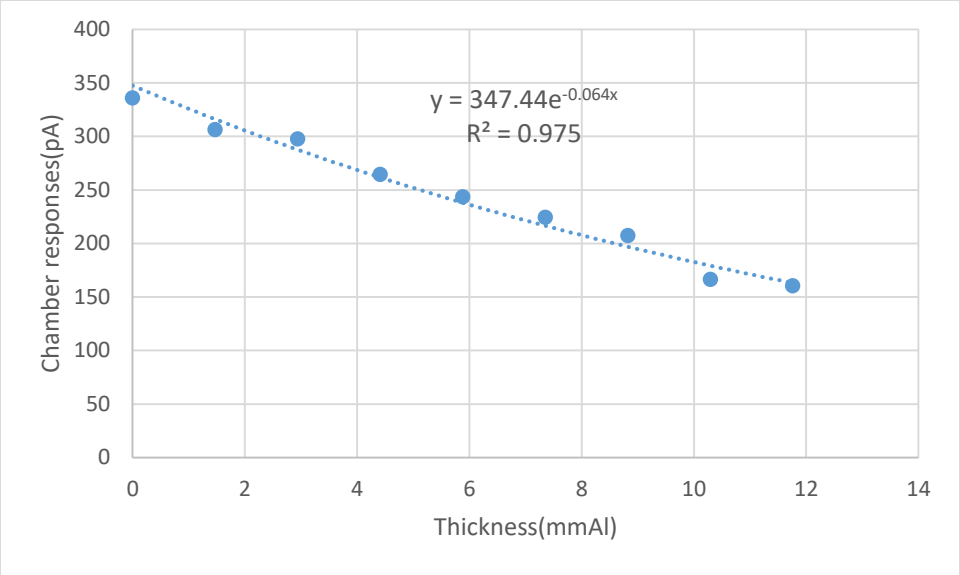

Figure 4.12: Chamber HVL response at 130 kVp.

From Table 4.11 and Figure 4.12, it can be concluded that at 120 kVp, the intensity of the beam decreases as the thickness increases till a point where all the beam will be attenuated. It can be concluded that an aluminium of 10.45 mm thick was used to attenuate the beam to half. .Therefore the HVL of the beam at 130 kVp is 10.45 mmAl.

4.3.8: Beam quality correction factor k_Q

The Beam quality correction factor k_Q was determined by using equation 2.11.

Table 4.12 shows normalized chamber beam quality correction factor k_Q at 100 kVp and HVL. Figure 4.13 presents a graph of normalized k_Q values and HVL.

Table 4.12: Normalized chamber beam quality correction factor K_Q and HVL

KVp	k_Q(mGy/pA^2)	Normalized k_Q Values	HVL(mmAl)
60	1.046	0.914	3.914
80	0.892	1.072	5.526
100	0.956	1.000	8.501
120	0.977	0.976	9.323
130	1.028	0.930	10.459

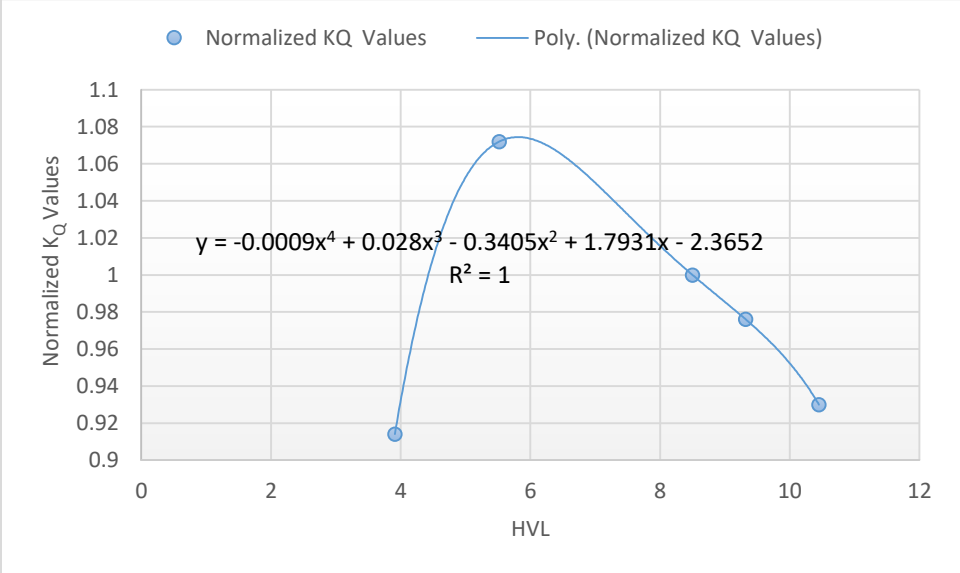

Figure 4.13: A graph of normalized k_Q values against HVL.

From the graph, the beam quality correction factor of the constructed chamber can expressed with a fourth degree polynomial equation in terms of HVL (in mmAl) using 100 KVp and 20 mAs (200 mA) as the reference exposure parameters.

4.3.9 Calibration coefficient of the constructed chamber

Table 4.13 shows the corrected parallel plate ionization chamber and the reference detector responses after cross calibration by substitution.

Table 4.13: Reference detector and chamber responses

Tube Voltage (KVp)	**Reference Detector Exposure (mGy)**	**Chamber response M_{corr} (pA)**
50	0.0336	18.0421
60	0.0692	38.9324
70	0.1146	78.5021
80	0.1723	113.6154
90	0.2424	153.5324
100	0.3188	196.1258
110	0.4057	250.9145
120	0.5153	310.3712
130	0.6219	355.9452

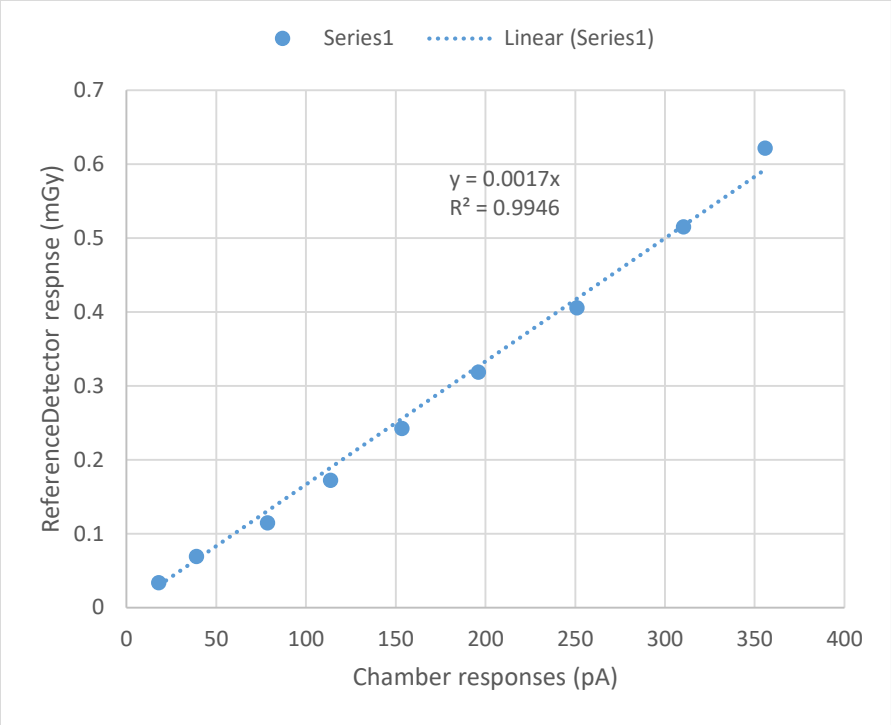

Figure 4.14: A graph of reference detector against chamber responses

The corrected responses for the reference detector and constructed chamber were used to determine the calibration coefficient of the local chamber using Equation 2.22. The results showed that the calibration coefficient N_k of the constructed chamber was $1.7x10^9$ mGy/A with uncertainty of ±0.01%. With a regression R^2 of 0.9946, the chamber response is linear to the detector response

4.4 Limitations

- Due to time constraints, and unavailability of a lower kVp X-ray source, like mammography machine, sensitivity test could not be done. Sensitivity test was to be done to find out the minimum energy required by the chamber to

give a signal.

- A solid state ionization chamber (Piranha multimeter) which was calibrated by Swedac Ackredictering was used for the cross calibration due to the non-existence of parallel plate ionization chamber in the country.

CHAPTER FIVE

CONCLUSIONS AND RECOMMENDATIONS

5.1 Conclusions

The ultimate goal of this work was to design and fabricate a portable, and less expensive parallel plate ionization chamber from available materials to minimize cost, a device that will assist medical physicist, radiographers, and radiation protection officers for dosimetry in conventional radiography in Ghana.

Indeed a vented parallel plate ionization chamber has been designed, fabricated, and calibrated for non calibrated beams and for scattered radiation. The results of the test highlighted some other important concepts of dosimetry, such as, angular/directional dependence, linearity, ion recombination, and leakage current.

The ion chamber was shown to be consistent, and capable of demonstrating some of the fundamental principles involved in ionizing radiation measurement.

The performance characteristics tests on bias voltage response, angular dependence, dose linearity check, HVL, pre-irradiation, current leakage, and energy dependence were all within tolerance limit of IEC 61674, 2013.

The calibration coefficient for the chamber was determined to be 1.7×10^{9} Gy/A with uncertainty of 0.01%.The chamber is applicable in X-ray beam quality ranging of 50 – 130 kVp. The chamber wall was made of Perspex (PMMA) which had given the chamber a unique property of tissue equivalence and also relatively less mechanical fragility.

Furthermore, the chamber has a maximum pre-leakage current of 3.35pA current which stabilizes after two minutes.

5.2 Recommendations

5.2.1 Radiography centres

The local vented parallel plate ionization chamber ionization chamber provides an alternative for dosimetric measurement of conventional X-ray machines and megavoltage x-ray beams. Facilities that are financially constrained to use commercial ionization chambers has a choice to make now.

5.2.2 Research community

- Test for sensitivity was not carried out since the Acuity simulator planning machine used has an energy range from 40 kVp to 150 kVp. There is the need to test for sensitivity to know the minimum kVp required to produce a signal.
- A similar test can be done by comparing the constructed chamber to another detector which calibration is based on ionization chamber.
- Although the chamber satisfies IEC 61674, 2013 recommendations, it is recommended that the calibration coefficient must be confirmed by a secondary standard dosimetry laboratory (SSDL)

REFERENCES

Ahmed, S. N. (2015). Physics and Engineering of Radiation Detection. Ontario, Canada: Academic Press Inc.

Alessandro, M. C., & Caldas, L. V. E., (2008), Plane-parallel ionization for X-radiation of conventional radiography and mammography, Radiol Bras vol.41 no.1 São Paulo

Almond, P. (2009). A brief history of dosimetry,calibration protocol, and the need for accuracy. AAPM Summer School.

Andreo, P. E. D. R. O., Seuntjens, J. P., & Podgorsak, E. B. (2005). Calibration of photon and electron beams Radiation Oncology Physics. Vienna: IAEA.

Andreo, P., Almond, P. R., Mattsson, O., Nahum A. E., And Roos, M. (1995). The Use Of Plane-Parallel Ionization Chambers In High-Energy Electron And Photon Beams, An International Code Of Practice For Dosimetry. IAEA Code of Practice for plane-parallel ionization chambers. Vienna: IAEA TRS-381.

Atix, F. H. (1986). Introduction to Radiological Physics and Radiation Dosimetry. Wisconsin: WILEY-VCH VerlagGmbH & Co.KGaA.

Bailey, D.L., Humm J.L., Todd-Pokropek, A., and Aswegen-van, A. (2014). Nuclear Medicine Physics: A Handbook for Teachers and Students. Vienna, Austria: IAEA.

Cherry, S. R., Sorenson, J. A., and Phelps, M. E. . (2012). Physics in Nuclear Medicine 4th . Elsevier Health Sciences.

De Souza C. N., Caldas L. V. E., Sibata, C. H., Ho, A. K., And Shin, K. H. (1995). Two New Parallel-Plate Ionization Chambers For Electron Beam Dosimetry. Pinheiros, Sao Paulo, S.P., Brazil 05499, 66.

DeWerd, L.A., Davis, S., Bartol, L., and Grenzow F. . (2006). Ionization Chamber Ionization Chamber Instrumentation. Wisconsin: University of Wisconsin & ADCL University of Wisconsin & ADCL Madison.

Goitein, M. (2007). Radiation Oncology: A Physicist's-Eye View. Windisch, Switzerland: Springer.

Halato, M. A., Suliman, I.I., Kafi, S. T., Ahmed, A. M., Sid Ahamed, F. A., Ibrahim, Z., and Suliman, M. F., (2008), Dosimetry for Patients undergoing Radiographic Examinations in Sudan . IX Radiation Physics & Protection Conference, Nasr City - Cairo, Egypt , 157-162.

Hartmann, G. H. (2012). Radiation Dosimeters. In J. Izewska, and G. Rajan. Review of Radiation Oncology Physics: A Handbook for Teachers and Students. (Heidelberg: IAEA.

Hooten, B. (2000). Ionization Chamber Construction. Standard Imaging, Inc.

IAEA, Technical Reports Series No. 398. (2000). Absorbed Dose Determination In External Beam Radiotherapy. Vienna - Austria: International Atomic Energy AgencY.

IAEA, Technical Reports Series No.457. (2007). Dosimetry In Diagnostic Radiology: An International Code Of Practice. Vienna, Austria: International Atomic Energy Agency.

IAEA-Tecdoc-1585. (2008). Measurement Uncertainty: A Practical Guide For Secondary Standards Dosimetry Laboratories. Measurement Uncertainty A Practical Guide For Secondary Standards Dosimetry Laboratories IAEA, Vienna, 2008 Austria: IAEA,.

IEC 61674 (2013). Medical electrical equipment — Dosimeters with ionization chambers and/or semiconductor detectors as used in X-ray diagnostic imaging. BSI Standards Publication. UK: BSI Standards Limited.

Inkoom S., Schandorf C., Emi-Reynolds G. and Fletcher J. J., (July 2011), Quality Assurance and Quality Control of Equipment in Diagnostic Radiology Practice - The Ghanaian Experience, Radiation Protection Institute, Ghana Atomic Energy Commission, Accra, https://www.researchgate.net/publication/221913318

Khan, F. M. (2010). Physics of Radiation Therapy, The, 4th Edition. Lippincott Williams & Wilkins.

Knoll, G. (2010). Radiation Detection and Measurement. 4th ed. New York, Wiley; .

Kyere, A. (2018). Lecture notes: Radiation Detection Principles and and Instruments. Radiological Protection. University of Ghana - Legon, Ghana: NET 130:.

Mayles, P., Nahum, A., & Rosenwald, J. C. (Eds.). (2007). Hand book of radiotherapy physics, theory and practice. Boca Raton,USA: CRC Press.

Okuno, E. (2012). Instrumentation for Dosimetry. In J. C. Hourdakis and R. Nowotny, Review of Diagnostic Radiology Physics: A Handbook for Teachers and Students. S. Paulo, Brazil,: IAEA.

Podgorsak, E. (2005). Radiation Oncology Physics: A Handbook for Teachers and Students. Vienna,Austria: International Atomic Energy Agency .

Podgorsak., E. (2006). Set of 189 slides on Calibration of Photon and Electron Beams. In E. a. Pdgorsak, Radiation Oncology Physics: A Handbook for Teachers and Students (p. 9.2.1 Slide 1). Montreal, McGill University: IAEA publication.

PTW Unidos Electrometer. (n.d.). ptwdosimetry.com. Retrieved from https://image.app.goo.gl/yQuZtTVCqvbC3wRe9

Ross, J. (2009). Design Of Ionization Chambers For Use In Teaching X-Ray Dosimetry . Oklahoma: East Central University.

Seco, J., Clasie, B., & Partridge, M. (2014). Review on the characteristics of radiation detectors for dosimetry and imaging. 59(20), R303. Physics in medicine and biology, 59(20) R303.

Solimanian, A., Ensaf, M. R., and Ghafoori,M. (2005). Design, Construction And Calibration Of Plane-Parallel Ionization Chambers At The SSDL Of Iran. Karaj - Iran: Atomic Energy Organization of Iran (AEOI).

Standard Imaging, Inc. (2015). Ionization Chamber And Leakage Measurements: Best Practice Guide. Standard Imaging, In.

APPENDIX 1.

1A: Ionization Chamber Assembly Design Drawings

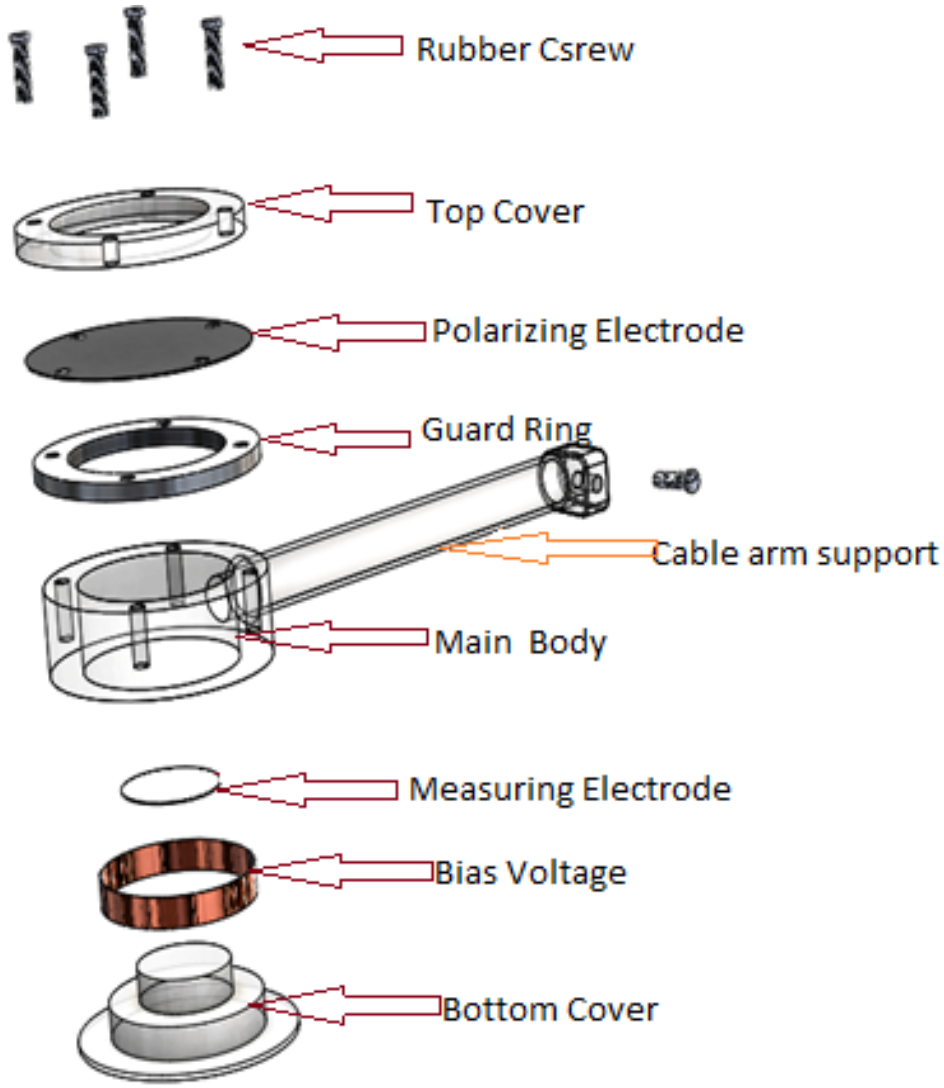

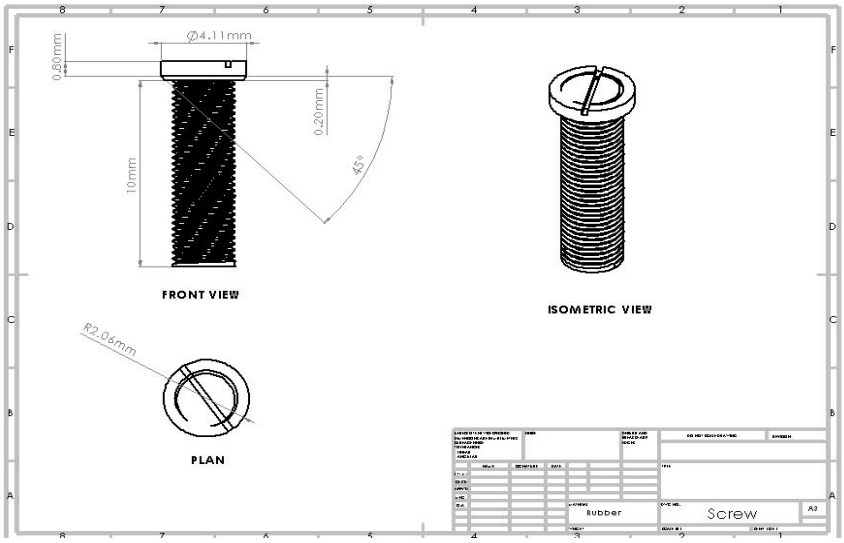

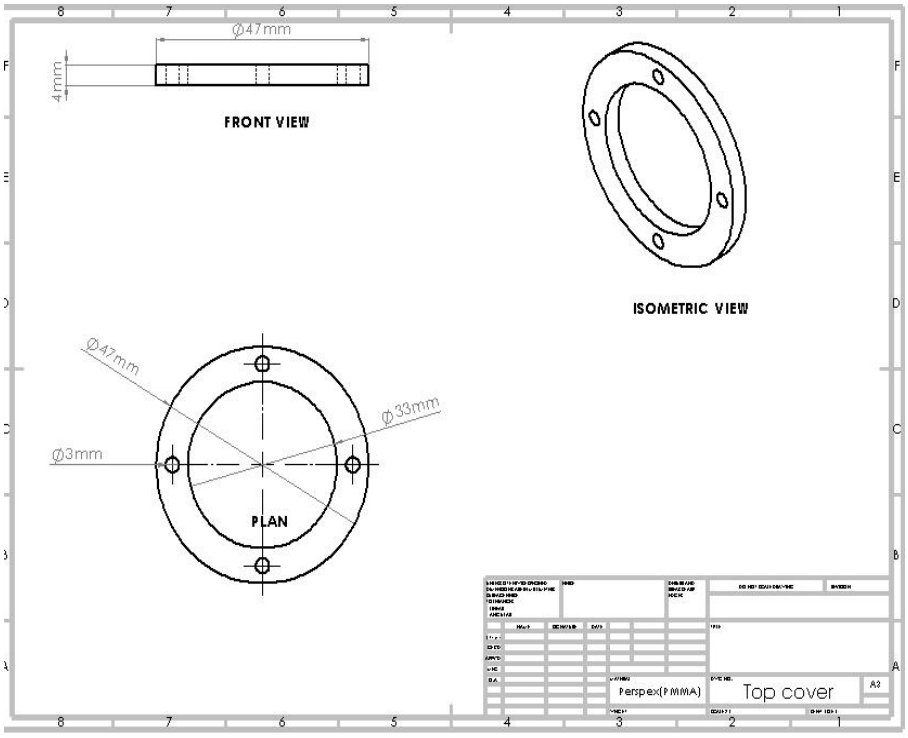

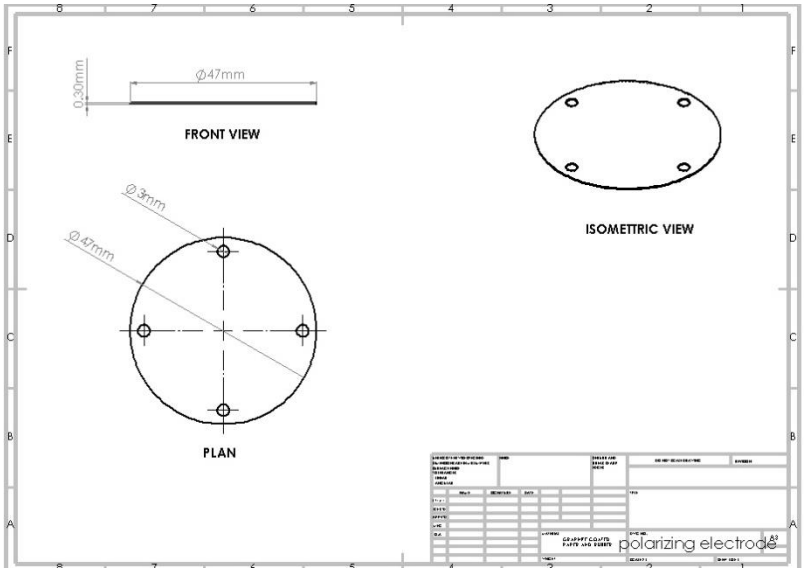

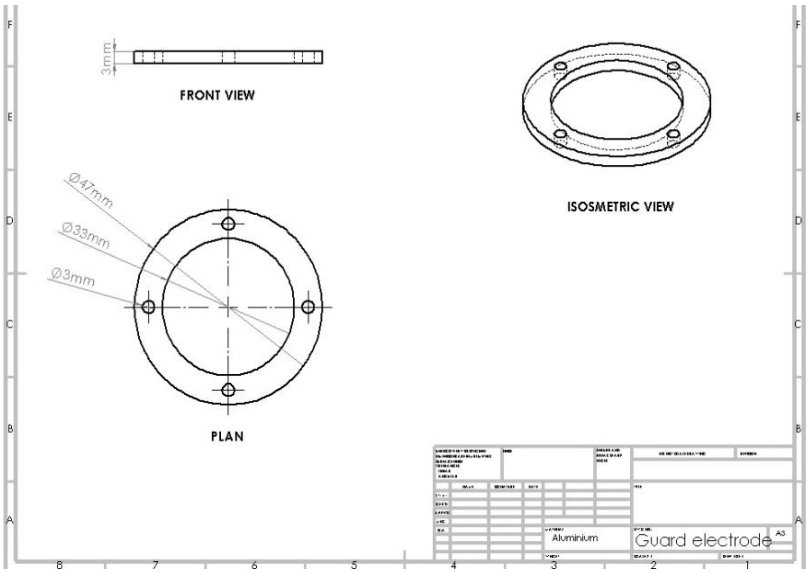

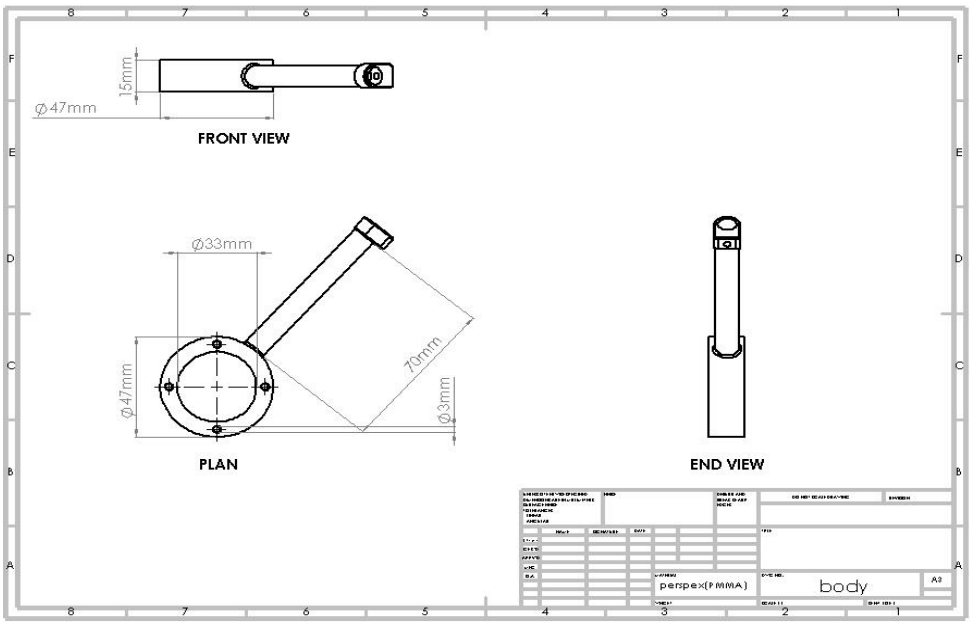

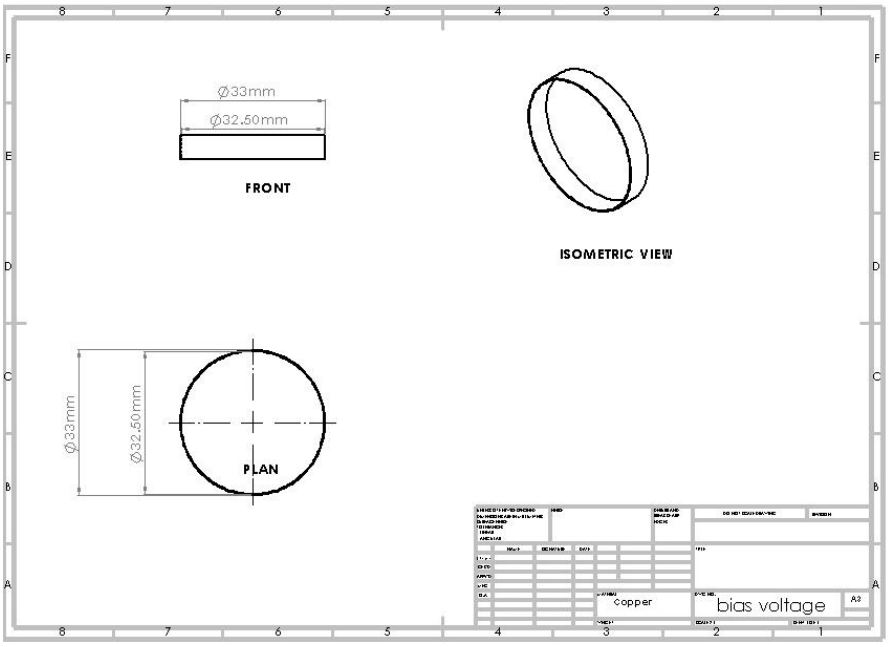

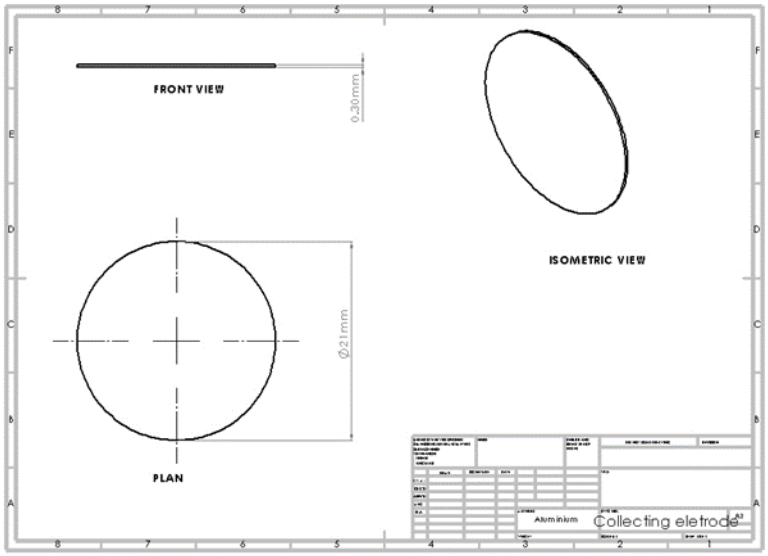

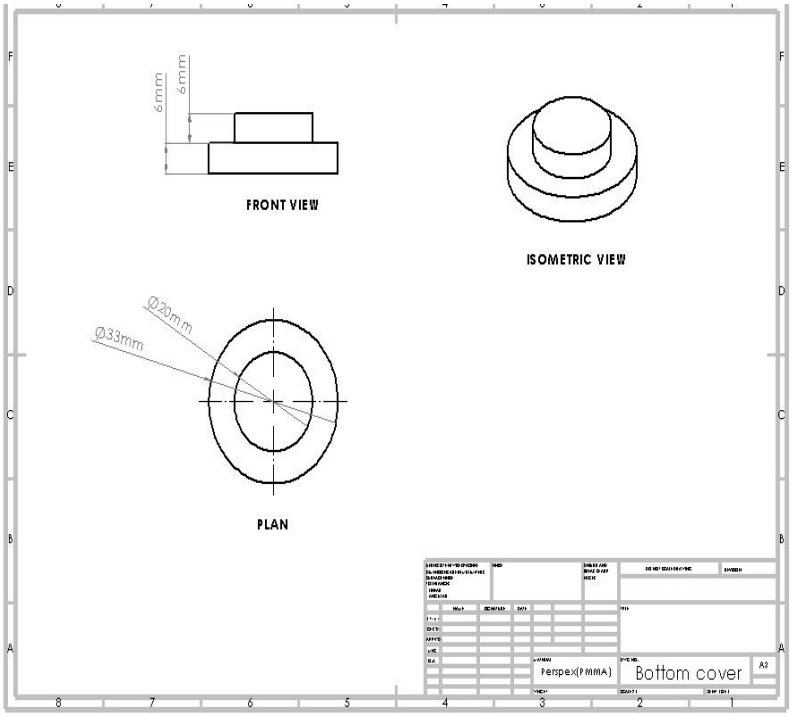

APPENDIX 2

Preliminary measurements of the parallel plate ionization chamber

Table 2A: Positive bias voltage electrometer readings for the chamber. (80KVP, 200mA and 20mAs)

Voltage (+V)	**Electrometer reading (pA)**	**P (hPa)**	**T (^{O}C)**	**K_{TP}**
50	91.7	1010.2	24.6	1.0187
100	105.4	1010.3	24.6	1.0186
150	114.6	1010.2	25.1	1.0204
200	115.5	1010.3	25.1	1.024
250	117.4	1010.3	24.7	1.0189
300	117.8	1010.1	24.7	1.0191
350	118.3	1010.1	24.6	1.0187
400	128.9	1010.1	24.6	1.0187

Voltage (-V)	Electrometer reading (pA)	P (hPa)	T (^{O}C)	K_{TP}
50	-86.4	1010.1	24.6	1.0188
100	-98.3	1010.1	24.6	1.0188
150	-102.5	1010.1	24.6	1.0188
200	-114.2	1010.3	25.0	1.0199
250	-110.7	1010.3	24.0	1.0199
300	-113. 1	1010.2	24.7	1.0190
350	-107.3	1010.2	24.7	1.0190
400	-103.7	1010.2	24.7	1.0190

Table 2B: Repeatability/Consistency electrometer readings for the chamber using a bias voltage of +300V and a setup of 80KVP, 200mA and 20mAs.

(KVp)	**Time (S)**	**Electrometer reading (pA)**	**Normalizes Values**
80	10	112.6	1.0000
80	20	113.1	0.9955
80	30	112.4	1.0017
80	40	111.4	0.9757
80	50	115.4	0.9757
80	60	114.6	0.9825
80	70	113.6	0.9911
80	80	110.4	1.0199
80	90	113.5	0.9920
80	100	114.2	0.9859
Mean		**113.12**	**Std Dev. 0.004227**

Table 2C: Corrected reproducibility electrometer readings for the chamber using a bias voltage of +300V in medium term stability

Date	**$M_{uncorr.}$ (pA)**	**P (hPa)**	**T (^{O}C)**	**K_{TP}**	**K_{pol}**	**$M_{corr.}$ (pA)**
25/09/2020	117.6	1010.5	26.1	1.023	0.9808	117.9
2/10/2020	112.6	1010.5	22.7	1.0119	0.9911	112.9
9/10/2020	114.3	1010.7	22.0	1.0093	0.9878	113.9

Table 2D: Temperature and pressure corrected electrometer readings for the chamber at different gantry angles normalized to the 0^o gantry angle response

Angle $^{(o)}$	**M_{uncorr} (pA)**	**K_{TP}**	**M_{corr}**	**Normalized to 0^o**
0	117.8	1.023	120.05	1.00000
10	113.9	1.023	116.51	0.96689
20	99.7	1.023	101.99	0.84634
30	98.3	1.023	100.56	0.834532
40	95.6	1.023	97.79	0.811544
50	93.7	1.019	95.48	0.79494
60	86.7	1.019	88.34	0.73311
70	84.7	1.020	86.39	0.71690
80	75.5	1.020	77.01	0.43903
90	55.5	1.019	56.55	0.46929
270	56.3	1.020	57.42	0.47652
280	77.4	1.020	78.94	0.66384
290	83.7	1.020	85.37	0.70844
300	87.5	1.020	89.25	0.74060
310	90.6	1.019	92.32	0.76609
320	91.7	1.019	93.44	0.77539
330	92.0	1.019	93.74	0.77593
340	93.4	1.019	95.17	0.78976
350	104.3	1.019	106.28	0.88193

Table 2E: Temperature and pressure corrected electrometer readings for the chamber response to different energy levels to determine current linearity.

(KVP)	M1	M2	M3	Mean M_{uncorr}	P (hPa)	T (^{O}C)	K_{TP}	$M_{corr.}$ (pA)
50	17.4	16.8	19.3	17.8	1010.5	22.7	1.0119	18.0
60	29.3	45.5	41.0	38.6	1010.6	22.1	1.0097	38.9
70	74.0	79.5	80.4	77.9	1010.7	21.9	1.0089	78.5
`80	121.4	117.7	98.8	112.6	1010.7	22.0	1.0093	113.6
90	168.8	149.5	138.4	152.2	1010.8	21.9	1.0088	153.5
100	195.4	197.4	190.6	194.4	1010.7	21.9	1.0089	196.1
110	258.9	245.3	242.3	248.8	1010.8	21.9	1.0088	250.9
120	321.4	322.5	278.5	307.4	1010.7	22.1	1.0096	310.3
130	336.4	356.4	365.5	352.7	1010.7	22.0	1.0093	355.9
140	368.2	369.4	396.5	378.0	1010.7	22.1	1.0096	381.6
150	384.2	465.3	454.6	434.7	1010.7	21.9	1.0089	438.5

Table 2F: Chamber response to different energy levels to determine HVL.

Voltage (KVP)	**M_{corr}**	**P1**	**P2**	**P3**	**P4**	**P5**	**P6**	**P7**	**P8**
60	38.9	37.2	31.5	19.5	9.7	--			
80	113.6	91.0	77.4	74.1	49.3	45.7	--		
100	196.1	189.3	167.6	153.4	130.0	117.5	105.9	91.7	--
120	310.3	283.4	274.3	234.4	218.3	197.4	150.1	135.5	--
130	355.9	306.3	297.7	264.5	243.5	124.5	207.5	166.4	160.4

NOTE: P1 means one piece of aluminium, plate, P2 means two pieces and in that order.

Table 2G: Piranha multi (Reference detector) KV reproducibility response.

R/N	KVp	Ref.Detector Response(mGy)
1	80	79.34
2	80	79.19
3	80	79.40
4	80	79.47
5	80	79.51
6	80	79.31
8	80	79.39
9	80	79.65
9	80	79.37
10	80	79.47

Table 2H: Piranha multi (Reference detector) response to different energy levels to determine the calibration coefficient.(KV Accuracy)

KVP	HVL (mmAl)	Total Filtr. (mmAl)	Exposure (mGy)
50	3.40	11.0	0.0336
60	4.09	9.6	0.0692
70	4.79	9.8	0.1146
80	5.42	9.7	0.1723
90	6.03	9.9	0.2424
100	6.59	10.0	0.3188
110	7.05	10.0	0.4057
120	7.52	10.0	0.5153
130	7.95	10.0	0.6219

Table 2I: Temperature and pressure corrected electrometer readings for the chamber response to different energy levels for cross calibration.

Voltage (KVP)	**M1**	**M2**	**M3**	**Mean M_{uncorr}**	**P (hPa)**	**T (^{O}C)**	**K_{TP}**	**$M_{corr.}$ (pA)**
50	17.4	16.8	19.3	17.8	1010.5	22.7	1.0119	18.0
60	29.3	45.5	41.0	38.6	1010.6	22.1	1.0097	38.9
70	74.0	79.5	80.4	77.9	1010.7	21.9	1.0089	78.5
`80	121.4	117.7	98.8	112.6	1010.7	22.0	1.0093	113.6
90	168.8	149.5	138.4	152.2	1010.8	21.9	1.0088	153.5
100	195.4	197.4	190.6	194.4	1010.7	21.9	1.0089	196.1
110	258.9	245.3	242.3	248.8	1010.8	21.9	1.0088	250.9
120	321.4	322.5	278.5	307.4	1010.7	22.1	1.0096	310.3
130	336.4	356.4	365.5	352.7	1010.7	22.0	1.0093	355.9
140	368.2	369.4	396.5	378.0	1010.7	22.1	1.0096	381.6
150	384.2	465.3	454.6	434.7	1010.7	21.9	1.0089	438.5

Table 2J: Chamber Pre irradiation current leakage response

(80 KVp,200 mA, 20 mAs abd 100 SSD)

Time (s)	**Chamber response (pA)**
10	6.85
20	5.60
30	5.00
40	4.70
50	4.45
60	4.30
70	4.05
80	3.45
90	3.40
100	3.35
110	3.25
120	3.30
Mean	4.308333